INTERNATIONAL STANDARD

ISO 15708-1

First edition
2002-06-01

Non-destructive testing — Radiation methods — Computed tomography —

Part 1: Principles

Essais non destructifs — Moyens utilisant les rayonnements — Tomographie informatisée —

Partie 1: Principes

Reference number
ISO 15708-1:2002(E)

ISO copyright office
Case postale 56 • CH-1211 Geneva 20
Tel. + 41 22 749 01 11
Fax + 41 22 749 09 47
E-mail copyright@iso.ch
Web www.iso.ch

Printed in Switzerland

Contents

Page

Foreword

ISO (the International Organization for Standardization) is a worldwide federation of national standards bodies (ISO member bodies). The work of preparing International Standards is normally carried out through ISO technical committees. Each member body interested in a subject for which a technical committee has been established has the right to be represented on that committee. International organizations, governmental and non-governmental, in liaison with ISO, also take part in the work. ISO collaborates closely with the International Electrotechnical Commission (IEC) on all matters of electrotechnical standardization.

International Standards are drafted in accordance with the rules given in the ISO/IEC Directives, Part 3.

The main task of technical committees is to prepare International Standards. Draft International Standards adopted by the technical committees are circulated to the member bodies for voting. Publication as an International Standard requires approval by at least 75 % of the member bodies casting a vote.

Attention is drawn to the possibility that some of the elements of this part of ISO 15708 may be the subject of patent rights. ISO shall not be held responsible for identifying any or all such patent rights.

ISO 15708-1 was prepared by Technical Committee ISO/TC 135, *Non-destructive testing*, Subcommittee SC 5, *Radiation methods*.

ISO 15708 consists of the following parts, under the general title *Non-destructive testing — Radiation methods — Computed tomography*:

— *Part 1: Principles*

— *Part 2: Examination practices*

Annex A forms a normative part of this part of ISO 15708.

Introduction

This part of ISO 15708 provides a tutorial introduction to the theory and use of computed tomography. It begins with an overview intended for the interested reader possessing a general technical background. Subsequent, more technical clauses describe the physical and mathematical basis of CT technology, the hardware and software requirements of CT equipment, and the fundamental measures of CT performance.

This part of ISO 15708 includes an extensive glossary (with discussions) of CT terminology and an extensive list of references to more technical publications on the subject. Most importantly, this part of ISO 15708 establishes consensus definitions for basic measures of CT performance, enabling purchasers and suppliers of CT systems and services to communicate unambiguously with reference to a recognized standard. It also provides a few carefully selected equations relating measures of CT performance to key system parameters.

Non-destructive testing — Radiation methods — Computed tomography —

Part 1: Principles

1 Scope

This part of ISO 15708 gives guidelines for, and defines terms for addressing the general principles of X-ray CT as they apply to industrial imaging. It also gives guidelines for a consistent set of CT performance parameter definitions, including how these performance parameters relate to CT system specifications.

2 Pre-amble

CT, being a radiographic modality, uses much the same vocabulary as other X-ray techniques. Because a number of terms have meanings or carry implications unique to CT, they appear with explanations in annex A. Throughout this part of ISO 15708, the term “X-ray” is used to denote penetrating electromagnetic radiation, however, electromagnetic radiation may be either X-rays or gamma rays.

3 Abbreviations

— BW beam width

— CDD contrast-detail-dose

— CT computed tomography

— CAT computerized axial tomography

— DR digital radiography

— ERF edge response function

— LSF line spread function

— MTF modulation transfer function

— NDE non-destructive evaluation

— PDF probability distribution function

— PSF point spread function

4 Requirements

4.1 Summary of computed tomography

Computed tomography (CT) is a radiographic method that provides an ideal examination technique whenever the primary goal is to locate and size planar and volumetric detail in three dimensions. Because of the relatively good penetrability of X-rays, as well as the sensitivity of absorption cross sections to atomic chemistry, CT permits the non-destructive physical and, to a limited extent, chemical characterization of the internal structure of materials. Also, since the method is X-ray based, it applies equally well to metallic and non-metallic specimens, solid and fibrous materials, and smooth and irregularly surfaced objects. When used in conjunction with other non-destructive evaluation (NDE) methods, such as ultrasound, CT data can provide evaluations of material integrity that cannot currently be provided non-destructively by any other means.

This part of ISO 15708 is intended to satisfy two general needs for users of industrial CT equipment:

a) the need for a tutorial document addressing the general principles of X-ray CT as they apply to industrial imaging;

b) the need for a consistent set of CT performance parameter definitions, including how these performance parameters relate to CT system specifications.

Potential users and buyers, as well as experienced CT inspectors, will find this part of ISO 15708 a useful source of information for determining the suitability of CT for particular examination problems, for predicting CT system performance in new situations and for developing and prescribing new scan procedures.

This part of ISO 15708 does not specify test objects and test procedures for comparing the relative performance of different CT systems; nor does it treat CT inspection techniques, such as the best selection of scan parameters, the preferred implementation of scan procedures, the analysis of image data to extract densitometric information or the establishment of accept/reject criteria for a new object.

Standard practices and methods are not within the purview of this part of ISO 15708. The reader is advised, however, that examination practices are generally part- and application-specific, and industrial CT usage is new enough that in many instances a consensus has not yet emerged. The situation is complicated further by the fact that CT system hardware and performance capabilities are still undergoing significant evolution and improvement. Consequently, an attempt to address generic examination procedures is eschewed in favour of providing a thorough treatment of the principles by which examination methods can be developed or existing ones revised.

The principal advantage of CT is that it non-destructively provides quantitative densitometric (i.e., density and geometry) images of thin cross sections through an object. Because of the absence of structural noise from detail outside the thin plane of inspection, images are much easier to interpret than with conventional radiographic data. The new user can learn quickly (often upon first exposure to the technology) to read CT data because the images correspond more closely to the way the human mind visualizes three-dimensional structures than conventional projection radiography. Further, because CT images are digital, they may be enhanced, analysed, compressed, archived, input as data into performance calculations, compared with digital data from other NDE modalities, or transmitted to other locations for remote viewing. Additionally, CT images exhibit enhanced contrast discrimination over compact areas. This capability has no classical analogue. Contrast discrimination of better than 0,1 % at three-sigma confidence levels over areas as small as one-fifth of one percent the size of the object of interest are common.

With proper calibration, dimensional inspections and absolute density determinations can also be made very accurately. Dimensionally, virtually all CT systems provide a pixel resolution of roughly 1 part in 1 000, and metrological algorithms, using *a priori* knowledge, can often measure dimensions to one-tenth of one pixel or so with three-sigma accuracies. Attenuation values can also be related accurately to material densities. If details in the image are known to be pure homogeneous elements, the density values may still be sufficient to identify materials in some cases. For the case in which no *a priori* information is available, CT densities cannot be used to identify unknown materials unambiguously, since an infinite spectrum of compounds can be envisioned that will yield any given observed attenuation. In this instance, the exceptional density sensitivity of CT can still be used to determine part morphology and highlight structural irregularities.

In some cases, dual energy (DE) CT scans can help identify unknown components. DE scans provide accurate electron density and atomic number images, providing better characterizations of the materials. In the case of known materials, the additional information can be traded for improved conspicuousness, faster scans or improved characterization. In the case of unknown materials, the additional information often allows educated guesses to be made as to the probable composition of an object.

CT, as a digital technique with data convertible to other formats, has proven valuable in the industrial application areas of rapid prototyping, reverse engineering and metrology. Rapid prototyping can be accomplished utilizing a class of manufacturing techniques where parts are built from computer models in a variety of materials. Stereolithography is one such technique that can utilize the thin slice information of CT to produce accurate polymer parts. Taking multiple CT slices, the two-dimensional images can be assembled to produce complete three-dimensional representations of scanned components. The data are presented to the stereolithography system as full volume information or simply contour plots, allowing the generation of either filled or hollow polymer parts. The choice of data would be based on the rapid tooling techniques that are applied in the specific application area.

CT-assisted reverse engineering methods are successful in enabling older designs without computer-aided design (CAD) files to access the many available rapid tooling techniques currently available. In reverse engineering applications, as in rapid prototyping, the two-dimensional images can be assembled to produce complete three-dimensional representations of scanned components. There are many computational methods that allow the CT-derived digital data to be transformed to a point cloud – a collection of points in 3-dimensional space that represent the surface of the part – or CAD contours, which can be used to reverse engineer the part. The CAD contours produced from CT data have been determined to be accurate to within a few thousandths of an inch. Thus, CT data are similar to dimensional data from coordinate measuring machines except they provide the following advantages:

a) CT data are acquired without contacting the part;

b) CT data not only provide surface information but also accurate measurements of all internal structures;

c) CT images can be formed of any object without special programming, regardless of its structural complexity.

Metrology of the CT data – evaluating dimensional measurements – can be accomplished using a number of techniques. Some examples of common techniques are direct measurement from the CT image data, measurement of the point cloud or registering the point cloud with the CAD model to produce a 3-D variance map. The deviations between the inspection data and the design data are evaluated based on the necessary tolerances for the application.

As with any modality, CT has its limitations. The most fundamental is that candidate objects for examination shall be small enough to be accommodated by the handling system of the CT equipment available to the user and radiometrically translucent at the X-ray energies used by that particular system. Further, CT reconstruction algorithms require that a full 180° of data be collected by the scanner. In some instances object size or opacity limits the amount of data that can be taken. While there are methods to compensate for incomplete data that produce diagnostically useful images, the resultant images are necessarily inferior to images from complete data sets. For this reason, complete data sets and radiometric transparency should be thought of as requirements. Current CT technology can accommodate attenuation ranges (peak-to-lowest-signal ratio) of approximately four orders of magnitude. This information, in conjunction with an estimate of the worst case chord through a new object and a knowledge of the average energy of the X-ray flux, can be used to make an educated guess on the feasibility of scanning a part that has not been examined previously.

Another potential drawback with CT imaging is the possibility of artifacts in the data. As used here, an artifact is anything in the image that does not accurately reflect true structure in the part being inspected. Because they are not real, artifacts limit the user's ability to quantitatively extract density, dimensional or other data from an image. Therefore, as with any technique, the user shall learn to recognize and be able to discount common artifacts subjectively. Some image artifacts can be reduced or eliminated with CT by improved engineering practice; others are inherent in the methodology. Examples of the former include scattered radiation and electronic noise. Examples of the latter include edge streaks and partial volume effects. Some artifacts are a little of both. A good example is the cupping artifact, which is due as much to radiation scatter (which can in principle be largely eliminated) as to the polychromaticity of the X-ray flux (which is inherent in the use of Bremsstrahlung sources).

Complete part examinations demand large storage capabilities or advanced display techniques or both and equipment to help the operator review the huge volume of data generated. This can be compensated for by state-of-the-art graphics hardware and automatic examination software to aid the user. However, automated accept/reject software is object dependent and to date has been developed and used in only a limited number of cases.

4.2 General description of computed tomography

CT is a radiographic inspection method that uses a computer to reconstruct an image of a cross-sectional plane (slice) through an object. The resulting cross-sectional image is a quantitative map of the linear X-ray attenuation coefficient, μ, at each point in the plane. The linear attenuation coefficient characterizes the local instantaneous rate at which X-rays are removed during the scan, by scatter or absorption, from the incident radiation as it propagates through the object (see clause 6). The attenuation of the X-rays as they interact with matter is a well-studied problem [20] and is the result of several different interaction mechanisms. For industrial CT systems with peak X-ray energy below a few MeV, all but a few minor effects can be accounted for in terms of the sum of just two interactions: photoelectric absorption and Compton scattering [20]. The photoelectric interaction is strongly dependent on the atomic number and density of the absorbing medium; the Compton scattering is predominantly a function of the electron density of the material. Photoelectric attenuation dominates at lower energies and becomes more important with higher atomic number, while Compton scattering dominates at higher energies and becomes more important at lower atomic number. In special situations, these dependencies can be used to advantage.

One particularly important property of the total linear attenuation coefficient is that it is proportional to material density, which is of course a fundamental physical property of all matter. The fact that CT images are proportional to density is perhaps the principal virtue of the technology and the reason that image data are often thought of as representing the distribution of material density within the object being inspected. This is a dangerous oversimplification however. The linear attenuation coefficient also carries an energy dependence that is a function of material composition. This feature of the attenuation coefficient may or may not (depending on the materials and the energies of the X-rays involved) be more important than the basic density dependence. In some instances, this effect can be detrimental, masking the density differences in a CT image; in other instances, it can be used to advantage, enhancing the contrast between different materials of similar density.

The fundamental difference between CT and conventional radiography is shown in Figure 1. In conventional radiography, information on the slice plane “P” projects into a single line, “A-A;” whereas with the associated CT image, the full spatial information is preserved. CT information is derived from a large number of systematic observations at different viewing angles, and an image is then reconstructed with the aid of a computer. The image is generated in a series of discrete picture elements or pixels. A typical CT image might consist of a 512 by 512 or 1024 by 1024 array of attenuation values for a single cross-sectional slice through a test specimen. This resultant two-dimensional map of the slice plane is an image of the test article. Thus, by using CT, one can, in effect, slice open the test article, examine its internal features, record the different attenuations, perform dimensional inspections and identify any material or structural anomalies that may exist. Further, by stacking and comparing adjacent CT slices of a test article, a three dimensional image of the interior can be constructed.

From Figure 1, it can be readily appreciated that if an internal feature is detected in conventional projection radiography, its position along the line-of-sight between the source and the film is unknown. Somewhat better positional information can be determined by making additional radiographs from several viewing angles and triangulating. This triangulation is a rudimentary, manual form of tomographic reconstruction. In essence, a CT image is the result of triangulating every point in the plane from many different directions.

Because of the volume of data that shall be collected and processed with CT, scans are usually made one slice at a time. A set of X-ray attenuation measurements is made along a set of paths projected at different locations around the periphery of the test article. The first part of Figure 2 illustrates a set of measurements made on a test object containing two attenuating discs of different diameters. The X-ray attenuation measurement made at a particular angle, ϕ_1, is referred to as a single view. It is shown as $f(x')$, where x' denotes the linear position of the measurement. The second part of Figure 2 shows measurements taken at several other angles $f(x')$. Each of the attenuation measurements within these views is digitalized and stored in a computer, where it is subsequently conditioned (e.g., normalized and corrected) and filtered (convolved), as discussed in more detail in clause 6. The next step in image processing is to back-project the views, which is also shown in the second part of Figure 2. Back-projection consists of projecting each view back along a line corresponding to the direction in which the projection data were collected. The back-projections, when enough views are used, form a faithful reconstruction of the object. Even in this simple example, with only four projections, the concentration of back-projected rays already begins to show the relative size and position of features in the original object.

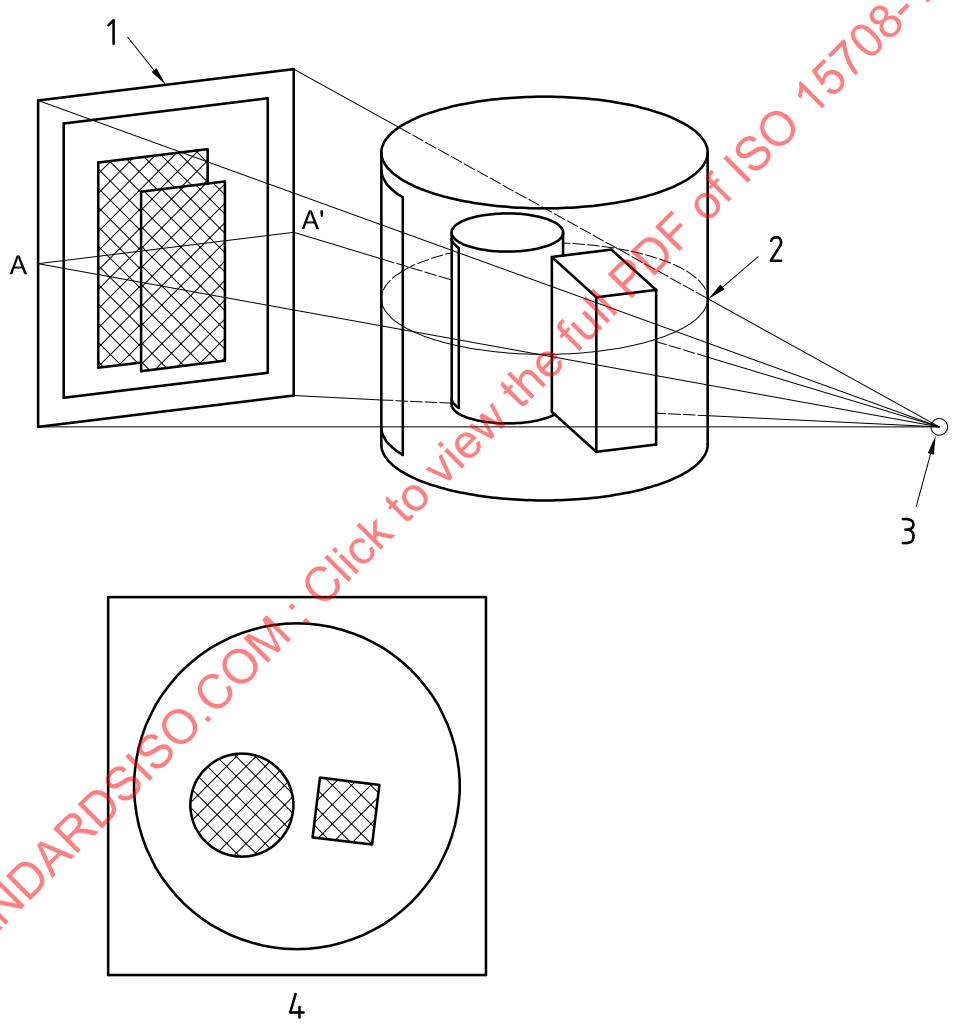

Key

1 Radiograph
2 Slice (plane P)
3 X-ray source
4 CT slice view (plane P)

Figure 1 — A CT image versus a conventional radiograph

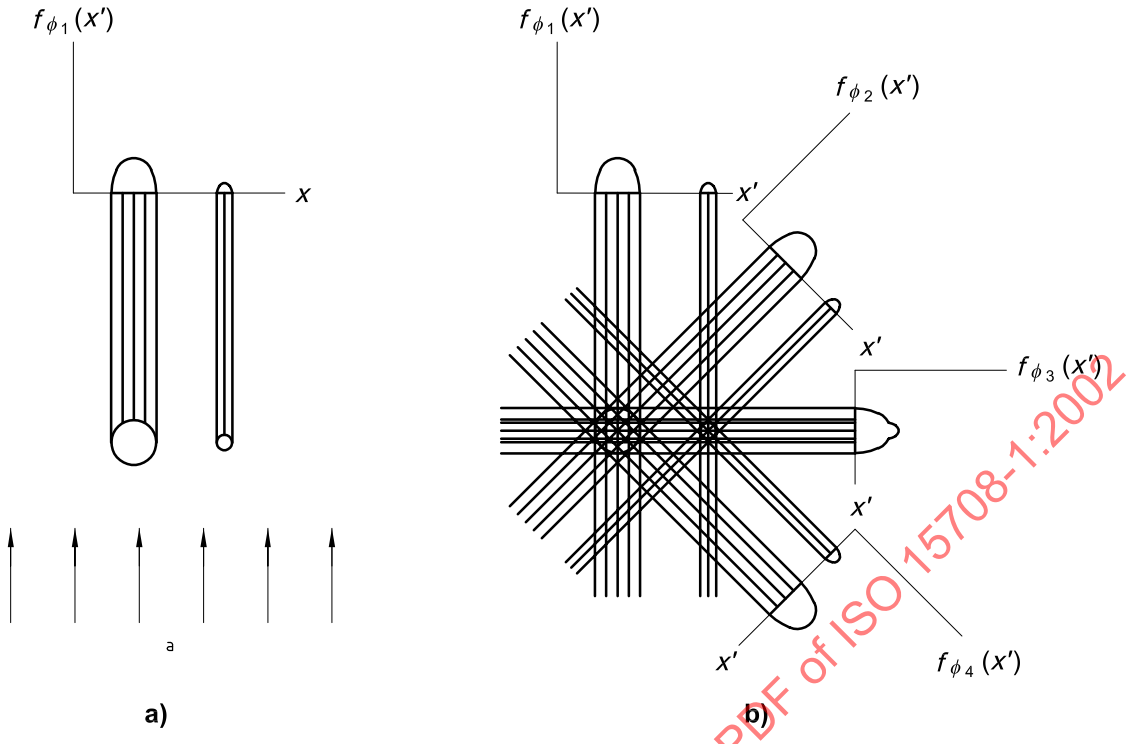

a Incident X-rays.

Figure 2 — Schematic illustrations of how CT works

4.3 System capability

4.3.1 General

The ability of a CT system to image thin cross-sectional areas of interest through an object makes it a powerful complement to conventional radiographic inspections. Like any imaging system, a CT system can never duplicate exactly the object that is scanned. The extent to which a CT image does reproduce the object is dictated largely by the competing influences of the spatial resolution, the statistical noise and the artifacts of the imaging system. Each of these aspects is discussed briefly here. A more complete discussion will be found in clauses 7 and 8.

4.3.2 Spatial resolution

Radiographic imaging is possible because different materials have different X-ray attenuation coefficients. In CT, these X-ray coefficients are represented on a display monitor as shades of grey, similar to a photographic image, or in false colour. The faithfulness of a CT image depends on a number of system-level performance factors, with one of the most important being spatial resolution. Spatial resolution refers to the ability of a CT system to resolve small details or locate small features with respect to some reference point.

Spatial resolution is generally quantified in terms of the smallest separation at which two points can be distinguished as separate entities. The limiting value of the spatial resolution is determined by the design and construction of the system and by the amount of data and sampling scheme used to interrogate the object of interest. The precision of the mechanical system determines how accurately the views can be back projected, and the X-ray optics determine the fineness of the detail that can be resolved. The number of views and the number of single absorption measurements per view determine the size of the reconstruction matrix that can be faithfully reconstructed. Reducing pixel size can improve spatial resolution in an image until the inherent limit set by these constraints is reached. Beyond this limit, smaller pixels do not increase the spatial resolution and can induce artifacts in the image. However, under certain circumstances, reconstructing with pixels smaller than would otherwise be warranted can be a useful technique. For instance, when performing dimensional inspections, working from an image with pixels as small as one-fourth the sample spacing can provide measurable benefit.

Other techniques to improve spatial resolution in specific regions of larger objects is known as region-of-interest (ROI) tomography [59], [68]. ROI tomography reconstructs a convex region within an object, utilizing a projection subset, on a specified sampling grid, providing higher resolution in this reduced area.

It can also be shown that a given CT image is equivalent to the blurring (convolution) of the ideal representation of the object with a smooth, two-dimensional Gaussian-like function called the point spread function (PSF). The specification of a system's PSF is an important characterization of a CT system and can be derived fairly accurately from the parameters of the CT system. The effect of the PSF is to blur the features in the CT image. This has two effects:

a) small objects appear larger;

b) sharp boundaries appear diffuse.

Blurring the image of small objects reduces resolution since the images of two small point-like objects that are close together will overlap and may be indistinguishable from a single feature. Blurring sharp edges reduces the perceptibility of boundaries of different materials for the same reason. This effect is especially important at interfaces between materials, where the possibility of separations of one type or another are of the greatest concern. Thus, knowledge of a CT system's PSF is crucial to the quantitative specification of the maximum resolution and contrast achievable with that system.

NOTE Since it is a common source of misunderstanding, that the smallest feature that can be detected in a CT image is not the same as the smallest that can be resolved. A feature considerably smaller than a single pixel can affect the pixel to which it corresponds to such an extent that it will appear with a visible contrast relative to adjacent pixels. This phenomenon, the “partial-volume effect,” is discussed in clause 6. The difference between the resolution of a small feature and the resolution of its substructure is of fundamental importance for CT.

4.3.3 Statistical noise

All images made from physical interactions of some kind will exhibit intrinsic statistical noise. In radiography, this noise arises from two sources:

a) intrinsic statistical variations due to the finite number of photons measured;

b) the particular form of instrumentation and processing used.

A good example in conventional radiography is film that has been underexposed. Even on a very uniform region of exposure, close examination of the film will reveal that only a small number of grains per unit area have been exposed. An example of instrumentation induced noise is the selection of coarser fine-grain film. If the films are exposed to produce an image with a given density, the fine-grain film will have lower statistical noise than the coarse-grain film. In CT, statistical noise in the image appears as a random variation superimposed on the CT number of the object. If a feature is small, it may be difficult to determine its median grey level and distinguish it from surrounding material. Thus, statistical noise limits contrast discrimination in a CT image.

Although statistical noise is unavoidable, its magnitude with respect to the desired signal can be reduced to some extent by attempting to increase the desired signal. This can be accomplished by increasing the scan time, the output of the X-ray source or the size of the X-ray source and detectors. Increasing the detector and source size, however, will generally reduce spatial resolution. This trade-off between spatial resolution and statistical noise is a fundamental characteristic of CT.

4.3.4 Artifacts

An artifact is something in an image that does not correspond to a physical feature in the test object. All imaging systems, whether CT or conventional radiography, exhibit artifacts. Examples of artifacts common to conventional radiography are blotches of underdevelopment on a film or scattering produced by high-density objects in the X-ray field. In both cases, familiarity with these artifacts allows the experienced radiographer to qualitatively discount their presence.

CT artifacts manifest themselves in diverse ways, since the CT image is calculated from a series of measurements. A common artifact is caused by beam hardening and manifests itself as cupping, i.e., a false radial gradient in the density that causes abnormally low values at the interior centre of a uniform object and high values at the periphery. Artifacts occurring at the interfaces between different density materials are more subtle. There is often an overshoot or undershoot in the density profile at such a density boundary. The interface density profile shall be well characterized so that delaminations or separations are not obscured. If the interface profile is not well characterized, false positive indications of defects or, more importantly, situations in which defects go undetected will result. Thus it is important to understand the class of artifacts pertinent to the inspection and to put quantitative limits on particular types of artifacts. Some of the artifacts are inherent in the physics and the mathematics of CT and cannot be eliminated. Others are due to hardware or software deficiencies in the design and can be eliminated by improved engineering.

The type and severity of artifacts are two of the factors that distinguish one CT system from another with otherwise identical specifications. The user shall understand the differences in these artifacts and how they will affect the determination of the variables to be measured. For instance, absolute density measurements will be affected severely by uncompensated cupping, but radial cracks can be visible with no change in detectability.

5 Apparatus

5.1 Subsystems

Modern CT systems, both industrial and medical, are composed of a number of subsystems, typically those shown in Figure 3.

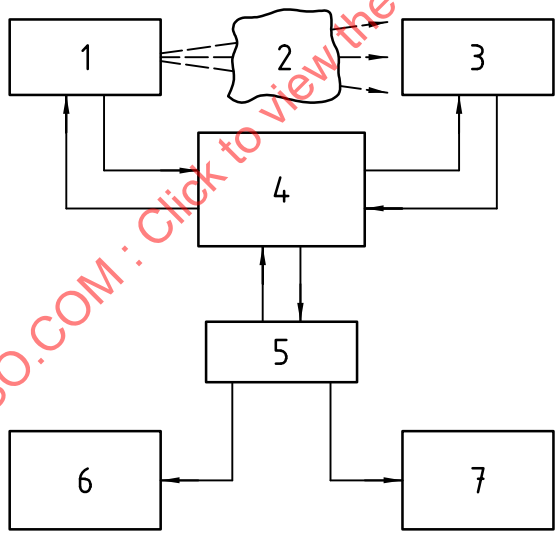

Key

1 Radiation source
2 Test object
3 Detectors
4 Mechanical assembly
5 Computer
6 Graphical display system
7 Data storage

Figure 3 — Typical components of a CT system

The choice of components for these subsystems depends on the specific application for which the system was designed; however, the function served by each subsystem is common in almost all CT scanners. These subsystems are:

a) an operator interface;

b) a source of penetrating radiation;

c) a radiation detector or an array of detectors;

d) a mechanical scanning assembly;

e) a computer system;

f) a graphical display system;

g) a data storage medium.

5.2 Operator interface

The operator interface defines what control the operator has over the system. From the perspective of the user, the operator interface is the single most important subsystem. The operator interface ultimately determines everything from the ease of use to whether the system can perform repetitive scan sequences. In short, the operator interface determines how the system is used.

5.3 Radiation sources

There are three rather broad types of radiation sources used in industrial CT scanners:

a) X-ray tubes;

b) linear accelerators;

c) isotopes.

The first two broad energy spectra are polychromatic or Bremsstrahlung electrical sources and the third is approximately monoenergetic radioactive sources. The choice of radiation source is dictated by precisely the same rules that govern the choice of radiation source for conventional radiographic imaging applications. A majority of existing CT scanners use electrical Bremsstrahlung X-ray sources either X-ray tubes or linear accelerators. One of the primary advantages of using an electrical X-ray source over a radioisotope source is the much higher photon flux possible with electrical radiation generators, which in turn allows shorter scan times. The greatest disadvantage of using an X-ray source is the beam hardening effect associated with polychromatic fluxes. Beam hardening results from the object preferentially absorbing low-energy photons contained in the continuous X-ray spectrum. Most medical scanners use as a source an X-ray tube operating with a potential of 120 kV to 140 kV. Industrial scanners designed for moderate penetrating ability also use X-ray tubes, but they usually operate at higher potentials, typically 200 kV to 400 kV. Systems designed to scan very massive objects, such as large rocket motors, use high-energy Bremsstrahlung radiation produced by linear accelerators. These sources have both high flux and good penetration, but they also have a broad continuous spectrum and the associated beam-hardening effect. Isotope sources are attractive for some applications. They offer an advantage over X-ray sources in that problems associated with beam hardening are nonexistent for the monoenergetic isotopes such as caesium^{137} and cobalt^{60}. They have the additional advantages, which are important in some applications, that they do not require bulky and energy-consuming power supplies, and they have an inherently more stable output intensity. The intensity of available isotopic sources, however, is limited by specific activity (photons/second/gram of material). The intensity affects signal-to-noise ratio and, even more importantly, the specific activity determines source spot size and thus spatial resolution. Both of these factors tend to limit the industrial application of isotopic scanners. Nevertheless, they can be used in some applications in which scanning time or resolution is not critical.

5.4 Radiation detectors

5.4.1 General

A radiation detector is used to measure the transmission of the X-rays through the object along the different ray paths. The purpose of the detector is to convert the incident X-ray flux into an electrical signal that can then be handled by conventional electronic processing techniques. The number of ray sums in a projection shall be comparable to the number of elements on the side of the image matrix. Such considerations result in a tendency for modern scanners to use large detector arrays that often contain several hundred to over a thousand sensors. There are essentially two general types of detectors in widespread use:

a) gas ionization detectors;

b) scintillation counters detectors.

5.4.2 Ionization detectors

In this type of transducer, the incoming X-rays ionize a noble element that may be in either a gaseous or, if the pressure is great enough, liquid state. The ionized electrons are accelerated by an applied potential to an anode, where they produce a charge proportional to the incident signal. Ionization detectors used in CT systems are typically operated in a current integration rather than pulse counting mode. In some embodiments of the technology, charge amplification can also be engineered. Ionization detectors are rugged and amenable to different implementations. A single detector enclosure can be segmented to create linear arrays with many hundreds of discrete sensors. Such detectors have been used successfully with 2 MV X-ray sources and show promise of being useful at higher energies as well.

5.4.3 Scintillation detectors

This type of transducer takes advantage of the fact that certain materials possess the useful property of emitting visible radiation when exposed to X-rays. By selecting fluorescent materials that scintillate in proportion to the incident flux and coupling them to some type of device that converts optical input to an electrical signal, sensors suitable for CT can be engineered. The light-to-electrical conversion can be accomplished in many ways. Methods include use of photodiodes, photo multiplier tubes or phosphor screens coupled to image capture devices (i.e. Charged Couple Displays (CCDs), video systems, etc.). Most recently, there are area detectors (panels) that provide a direct capture technique, utilizing amorphous silicon or amorphous selenium photo-conductors with a phosphor coating, which directly convert incident radiation into electrical charge. Like ionization detectors, scintillation detectors afford considerable design flexibility and are quite robust. Scintillation detectors are often used when very high stopping power, very fast pulse counting, or areal sensors are needed. Recently, for high-resolution CT applications, scintillation detectors with discrete sensors have been reported with array spacings in the order of 25 µm. Both ionization and scintillation detectors require considerable technical expertise to achieve performance levels acceptable for CT.

5.5 Mechanical scanning equipment

Mechanical equipment provides the relative motion between the test article, the source and the detectors. It makes no difference, at least in principle, whether the test object is systematically moved relative to the source and detectors, or if the source and detectors are moved relative to the test object. Physical considerations such as the weight or size of the test article shall be the determining factors for the most appropriate motion to use.

The majority of scan geometries that have been used can be classified as one of the following five generations. This classification is a legacy of the early, rapid development of CT in the medical arena and is reviewed here because these terms are still widely used. The distinctions between the various scan geometries are illustrated in Figure 4.

First-generation CT systems are characterized by a single X-ray source and single detector that undergo both linear translation and rotational motions. The source and detector assembly is translated in a direction perpendicular to the X-ray beam. Each translation yields a single view, as shown in Figure 2. Successive views are obtained by rotating the test article and translating again. The advantages of this design are simplicity, good view-to-view detector matching, flexibility in the choice of scan parameters (such as resolution and contrast), and ability to accommodate a wide range of different object sizes. The disadvantage is a longer scanning time.

Second-generation CT systems use the same translate/rotate scan geometry as the first generation. The primary difference is that second-generation systems use a fan beam of radiation and multiple detectors so that a series of views can be acquired during each translation, which leads to correspondingly shorter scan times. Like first-generation systems, second-generation scanners have the inherent flexibility to accommodate a wide range of different object sizes, which is an important consideration for some industrial CT applications.

Third-generation CT systems normally use a rotate-only scan geometry, with a complete view being collected by the detector array during each sampling interval. To accommodate objects larger than the field of view subtended by the X-ray fan, it is possible to include part translations in the scan sequence, but data are not acquired during these translations as during first or second-generation scans. Typically, third-generation systems are faster than their second-generation counterparts; however, because the spatial resolution in a third-generation system depends on the size and number of sensors in the detector array, this improvement in speed is achieved at the expense of having to implement more sensors than with earlier generations. Since all elements of a third-generation detector array contribute to each view, rotate-only scanners impose much more stringent requirements on detector performance than do second-generation units, where each view is generated by a single detector.

Fourth-generation CT systems also use a rotate-only scan motion. The difference between third-generation and fourth-generation systems is that a fourth-generation CT system uses a stationary circular array of detectors and only the source moves. The test specimen is placed within the circle of detectors and is irradiated by a wide fan beam which rotates around the test article. A view is made by obtaining successive absorption measurements of a single detector at successive positions of the X-ray source. The number of views is equal to the number of detectors. These scanners combine the artifact resistance of second-generation systems with the speed of third-generation units, but they can be more complex and costly than first-, second-, or third-generation machines, they require that the object fit within the fan of X-rays, and they are more susceptible to scattered radiation.

Fifth-generation CT systems are different than the previous modes, in that there is no mechanical motion involved. The scanner uses a circular array of X-ray sources, which are electronically switched on and off. The sources project on to a curved fluorescent screen, so that when an X-ray source is switched on, a large volume of the part is imaged simultaneously, providing projection data for a cone beam of rays diverging from the source. This method of data collection is essentially different from the other four, since a series of two-dimensional projections of a three-dimensional object is collected rather than a series of one-dimensional projections of a two-dimensional object. This scanning mode is appropriate for precise imaging of a rapidly moving part (typical application is imaging of the heart or other moving organs).

A significant factor in driving medical CT systems to use rotate-only scan geometries was the requirement that scanning times be short compared to the length of time that a patient can remain motionless or that involuntary internal motion can be ignored (that is, seconds). These considerations are not as important for industrial applications in which scan times for specific production-related items can typically be much longer (that is, minutes) and the dose to the object is often not an important factor. A second-generation scan geometry is attractive for industrial applications in which a wide range of part sizes must be accommodated, since the object does not have to fit within the fan of radiation as it generally does with third- or fourth-generation systems. A third-generation scan geometry is attractive for industrial applications in which the part to be examined is well defined and scan speed is important. To date, first-, fourth-, and fifth-generation scan geometries have seen little commercial application, but there may be special situations for which they would be well suited.

5.6 Computer systems

The computer system(s) performs two major tasks: 1) controlling the scan motion, source operation, and data acquisition functions; and 2) handling the reconstruction, image display and analysis, and data archival and retrieval functions. Most modern CT systems partition these functions between separate dedicated microprocessors. Image formulation operations involve intensive computation, and they are almost always performed with array processors and specially designed hardware.

5.7 Image display and processings

Image display and processing are subfunctions of the computer system that provide a degree of image interaction not available with conventional radiography. The mapping between the pixel linear attenuation coefficient and the displayed intensity of the pixel can be changed to accommodate the best viewing conditions for a particular feature. Image processing functions such as statistical and densitometric analyses can be performed on an image or group

of images. The digital nature of the image allows major advances in the way data are processed, analysed and stored. This process of mapping reconstructed pixel values to displayed pixel values is shown in Figure 5.

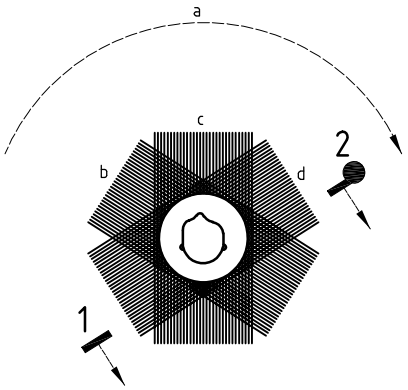

a) 1st generation single pencil beam translate/rotate scanner

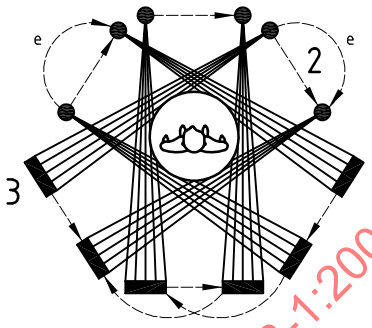

b) 2nd generation multiple pencil beam translate/rotate scanner

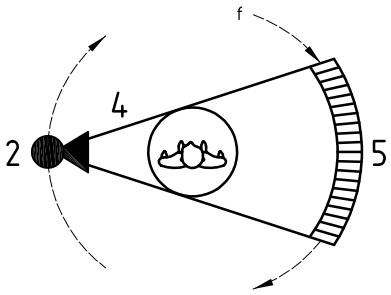

c) 3rd generation rotate/rotate fan beam scanner

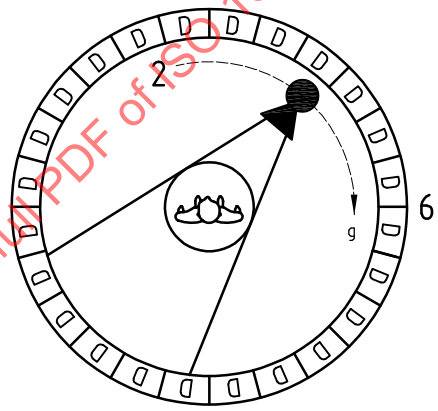

d) 4th generation rotate/stationary inverted fan beam scanner

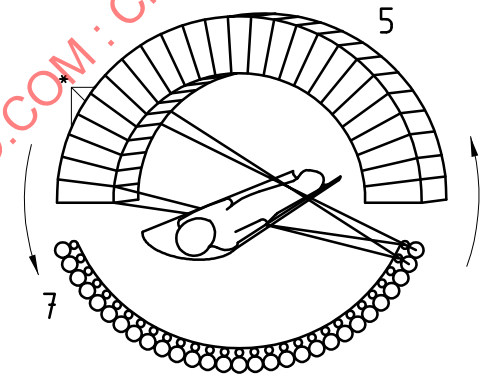

e) 5th generation cone beam "cylindrical" scanner

Key

1	Detector	4	Pulsed fan beam
2	X-ray tube	5	Detector array
3	Multiple detectors	6	Stationary detector array
		7	X-ray sources

a	1° increments	e	Multiple degree increments.
b	1st scan.	f	360° continuous sweep.
c	60th scan.	g	Direction of motion.
d	120th scan.		

Figure 4 — Five sketches illustrating the evolution of medical CT scan geometries; each embodiment is representative of a distinct generation of instrumentation

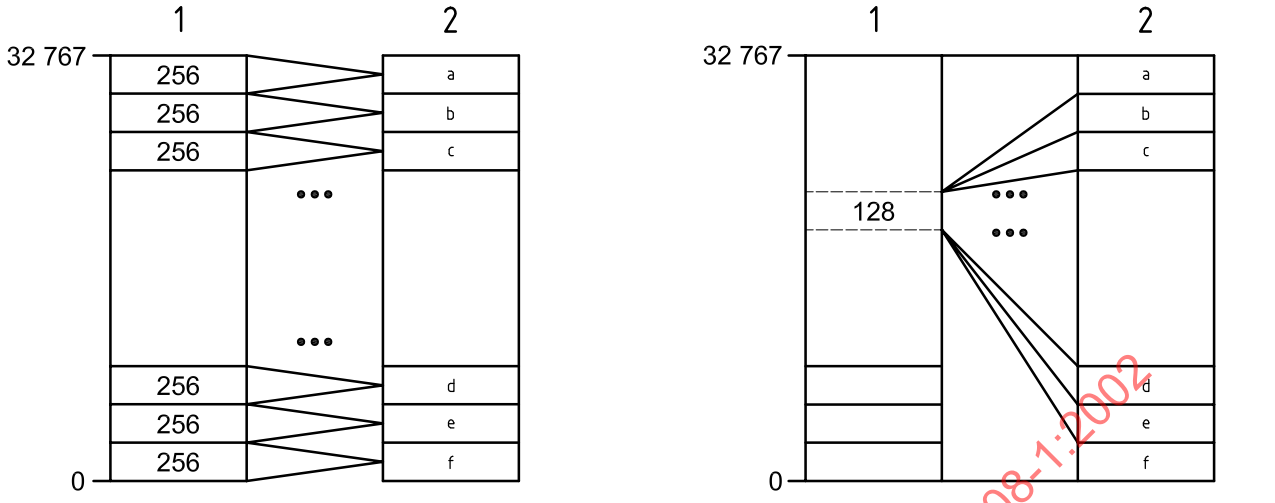

a) maximum image latitude **b) maximum contrast over a narrow range of contrast**

Key

1 Image

2 Display colours ([a] white; [b] grey; [c] blue; [d] violet; [e] purple; [f] black)

Figure 5 — Conceptual illustration of the process of mapping a large range of image values on to a much smaller range of displayable values

5.8 Archival data storage

Information such as image data, operating parameters, part identification, operator comments, slice orientation, and other data is usually saved (archived) in a computer-readable, digital format on some type of storage medium (e.g., magnetic tape, floppy disk or optical disk). The advantage of saving this material in computer-readable format rather than in simple hardcopy form is that it would take dozens of pictures of each slice at different display conditions to approximate the information contained in a single CT image. Also, images of samples made with old and new data sets can be compared directly, and subsequent changes in reconstruction or analysis procedures can be reapplied to saved data or images. Also, as discussed in 4.1, CT, as a digital technique, has proven valuable in the industrial application areas of rapid prototyping, reverse engineering and metrology. Each of these applications requires the storage and conversion of the CT image data.

5.9 Summary of apparatus

These elements are the basic building blocks of any CT system. Each CT system will have its own particular set of features. It is the responsibility of the user to understand these differences and to select the system most appropriate for the intended application.

6 Theoretical background

6.1 X-ray interactions

Penetrating radiation is classified according to its mode of origin. Gamma-rays are produced by nuclear transitions and emanate from the atomic nucleus. Characteristic X-rays are produced by atomic transitions of bound electrons and emanate from the electronic cloud. Continuous X-rays, or Bremsstrahlung, are produced by the acceleration or deceleration of charged particles, such as free electrons or ions. Annihilation radiation is produced by the combination of electron-positron pairs and their subsequent decomposition into pairs of photons. All evidence suggests that the interaction of these photons with matter is independent of their means of production and is dependent only on their energy. For this reason, this part of ISO 15708 refers to penetrating radiation in the energy range from a few keV to many MeV as X-rays, regardless of how they are produced.

X-rays can in theory interact with matter in only four ways: they can interact with atomic electrons; they can interact with nucleons (bound nuclear particles); they can interact with electric fields associated with atomic electrons and/or atomic nuclei; they can interact with meson fields surrounding nuclei. In theory, an interaction can result in only one of three possible outcomes: the incident X-ray can be completely absorbed and cease to exist; the incident X-ray can scatter elastically; the incident X-ray can scatter inelasitcally. Thus, in principle, there are twelve distinct ways in which photons can interact with matter, see Table 1. In practice, all but a number of minor phenomena can be explained in terms of just a few principal interactions. These are listed in Table 1. Some of the possible interactions have yet to be physically observed.

Table 1 — X-ray interactions with matter

Matter	Effects of interaction		
	Complete absorption	Elastic scattering	Inelastic scattering
Atomic electrons	Photoelectric effect	Rayleigh scattering	Compton scattering
Nucleons	Photo disintegration	Thomson scattering	Nuclear resonance scattering
Electric field of atom	Pair production	Delbruck scattering	Not observed
Meson field of nucleus	Meson production	Not observed	Not observed

The photon-matter interactions of primary importance to radiography are the ones which dominate observable phenomena: photoelectric effect, Compton scattering and pair production. Their domains of relative importance as a function of photon energy and material atomic number are shown in Figure 6. At energies below about 1 MeV, pair production is not allowed energetically and X-ray interactions with matter are dominated by processes involving the atomic electrons. Of the other possible interactions (see Table 1) Rayleigh scattering is typically small but non-negligible. The rest are either energetically forbidden or insignificant. At energies above 1 MeV, pair production is energetically allowed and competes with Compton scattering. Of the other possible interactions, photo disintegration is typically negligible in terms of measurable attenuation effects but at energies above about 8 MeV can lead to the production of copious amounts of neutrons. The rest of the interactions are either energetically forbidden or insignificant.

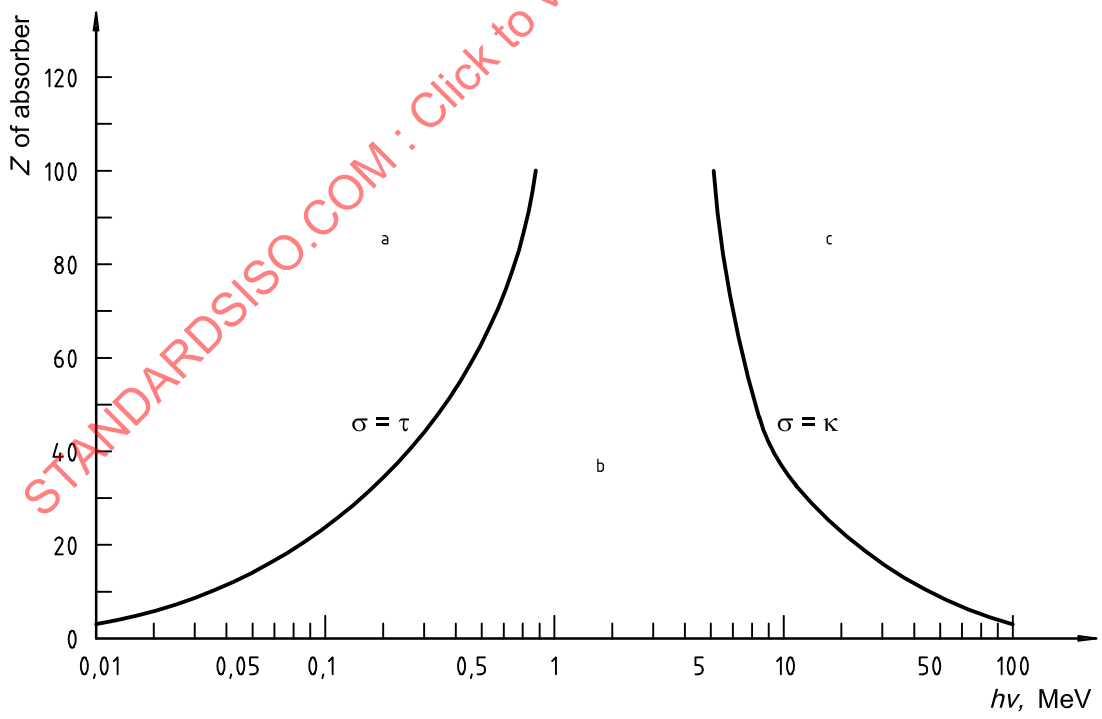

a Photoelectric effect dominant.

b Compton effect dominant.

c Pair production dominant.

Figure 6 — Principal X-ray interactions

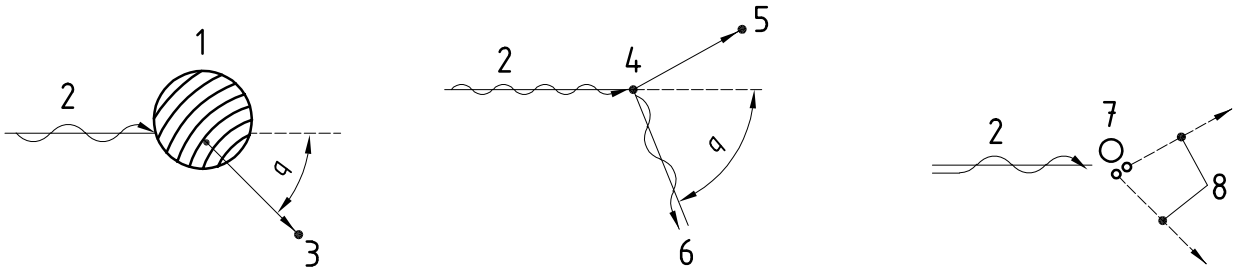

a) photoelectric effect b) compton scattering c) pair production

Key

1	Atom	4	Atomic electron	7	Atomic nucleus
2	Incident photon	5	Compton electron	8	Electron pair
3	Photoelectron	6	Compton scattered electron		

Figure 7 — X-ray interaction mechanisms

The three principal interactions are schematically illustrated in Figure 7. With the photoelectric effect [Figure 7a)], an incident X-ray interacts with the entire atom as an entity and is completely absorbed. To conserve energy and momentum, the atom recoils and a bound electron is ejected. Although the subsequent decay processes lead to the generation of characteristic X-rays and secondary electron, these are not considered part of the photoelectric effect. As can be seen from Figure 6, the photoelectric effect predominates at low energies and high atomic numbers.

With Compton scattering [Figure 7b)], an incident X-ray interacts with a single electron (which, practically speaking, is almost always bound) and scatters inelastically, meaning the X-ray loses energy in the process. This type of scattering is often referred to as incoherent scattering, and the terms are used interchangeably. To conserve energy and momentum, the electron recoils and the X-ray is scattered in a different direction at a lower energy. Although the X-ray is not absorbed, it is removed from the incident beam by virtue of having been diverted from its inital direction. The vast majority of background radiation in and around radiographic equipment is from Compton-scattered X-rays. As can be seen from Figure 6, Compton scattering predominates at intermediate energies, more or less independently of atomic number.

With pair production [Figure 7c)], an incident X-ray interacts with the strong electric field surrounding the atomic nucleus and ceases to exist, creating in the process an electron-positron pair. Energy and momentum are conserved by the emerging pair of particles. Although the positrons eventually interact with electrons, generating annihilation radiation, this secondary effect is not considered part of the pair production process. As can be seen from Figure 6, pair production predominates at high energies and high atomic numbers.

6.2 Computed tomography technical background

CT is the science of recovering an estimate of the internal structure of an object from a systematic, non-destructive interrogation of some aspect of its physical properties. Generally, but not always[70], the problem is kept manageable by limiting the task to a determination of a single image plane through the object. If three-dimensional information is required, it is obtained by comparing and, if necessary, resectioning[22] contiguous cross-sections through the object of interest.

In its most basic form, the CT inspection task consists of measuring a complete set of line integrals involving the physical parameter of interest over the designated cross-section and then using some type of computational prescription, or algorithm, to recover an estimate of the spatial variation of the parameter over the desired slice. In order to best illustrate the basic principles of CT, the discussion limits itself to the examination problem of determining a single image plane through an object. Separate clauses focus on what constitutes an acceptable CT data set; a way in which such a data set can be collected; some of the competing effects that limit performance in practice. The discussion of the companion task of image reconstruction limits itself to the problem of reconstructing a single two-dimensional image; three-dimensional reconstructions are not discussed. The treatment includes the goal of the reconstruction process and one way in which CT data can be reconstructed.

The task of obtaining a useable data set and the companion problem of how these data are then reconstructed to produce an image of the object are reviewed in 6.4 to 6.7.

6.3 Radon transform

The theoretical mathematical foundation underlying CT was established in 1917 by J. Radon[65]. Motivated by certain problems of gravitational physics, Radon established that if the set of line integrals of a function, which is finite over some region of interest and zero outside it, is known for all ray paths through the region, then the value of the function over that region can be uniquely determined. A particular function and its associated set of line integrals form a transform pair; the set of integrals is referred to as the Radon transform of the function. Radon demonstrated the existence of an inverse transform for recovering a function from its Radon transform, providing an important existence theorem for what later came to be called CT. Over the years, the process of recovering a function from its Radon transform has been rediscovered numerous times[9], [16], [18], [49], [62].

In a classic example of the old principle that “like equations have like solutions” tomography has been demonstrated using many different physical modalities to obtain the necessary line integrals of some physical parameter. Objects ranging in size from bacteriophages[77] to supernova[58] have been studied tomographically using a wide variety of physical probes, including X-rays (medical CAT scanners or simple X-ray CT)[12], [61], sound waves (ultrasonic imaging)[26], [67], electromagnetic fields (NMR, or, more commonly now, MR imaging),[50], ionizing particles[1], [32] and biologically active isotopes (SPECT and PET scanners)[13], [48], [82]. These methods have been used to study many types of material properties, such as X-ray attenuation, density, atomic number, isotopic abundance, resistivity, emissivity and, in the case of living specimens, biological activity.

The essential technological requirement, and that which these various methods have in common, is that a set of systematically sampled line integrals of the parameter of interest be measured over the cross-section of the object under inspection and that the geometrical relationship of these measurements to one another be well known. Within this constraint many different methods of collecting useful data exist, even for the same imaging modality. However, the quality of the resulting reconstruction depends on at least three major factors:

a) how finely the object is sampled;

b) how accurately the individual measurements are made;

c) how precisely each measurement can be related to an absolute frame of reference.

6.4 Sampling the Radon transform

Given this general background, the discussion here now focuses on the specific task of tomographic imaging using X-rays as the inspection modality. For monoenergetic X-rays, attenuation in matter is governed by Lambert's law of absorption [29], which holds that each layer of equal thickness absorbs an equal fraction of the radiation that traverses it. Mathematically, this can be expressed as the following:

$$\frac{\mathrm{d}I}{I} = -\mu \times \mathrm{d}x \qquad (1)$$

where:

$\mathrm{d}I/I$ is the fraction of radiation removed from the flux as it traverses a small thickness, $\mathrm{d}x$, of material;

I is the intensity of the incident radiation in watt per steradian;

μ is the constant of proportionality.

In the physics of X-ray attenuation, μ is referred to as the linear absorption coefficient. Equation (1) can be integrated easily to describe X-ray attenuation in the following perhaps more familiar form[20]:

$$I = I_0 \times \mathrm{e}^{-\mu x} \qquad (2)$$

where

I_0 is the intensity of the unattenuated radiation in watt per steradian;

I is the intensity of the transmitted flux after it has traversed a layer of material of thickness x.

If X-rays penetrate a non-homogeneous material, equation (2) shall be rewritten in the more general form:

$$I = I_0 \times \mathrm{e}^{-\int \mu(s)\mathrm{d}s} \tag{3}$$

where the line integral is taken along the direction of propagation and $\mu(s)$ is the linear absorption coefficient at each point on the ray path. In X-ray CT, the fractional transmitted intensity, I/I_0, is measured for a very large number of ray paths through the object being inspected and is then logged to obtain a set of line integrals for input to the reconstruction algorithms. Specifically, the primary measurements, I and I_0, are processed, often "on the fly," to obtain the necessary line integrals:

$$\int \mu(s) \times \mathrm{d}s = -\ln(I / I_0) \tag{4}$$

To obtain an adequate measure of the line integrals, highly collimated pencil beams of X-rays are used to make the measurements of the fractional transmittance. In the terminology of CT, the set of line integrals resulting from a scan of an object can be grouped conceptually into subsets referred to as views. Each view corresponds to a set of ray paths through the object from a particular direction (see Figure 8). The views are also referred to as projections or profiles, while each individual datum within a given projection is referred to as a sample or often simply a data point.

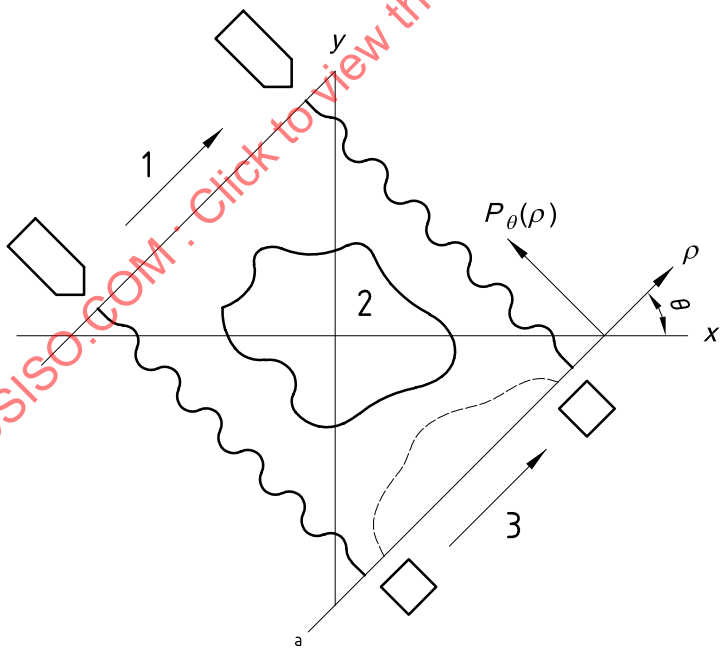

Key

1 X-ray tube
2 Object
3 Detector
a Direct space

Figure 8 — Schematic illustration of basic CT scan geometry showing a single profile consisting of many discrete samples

As previously indicated, the reconstruction problem places a number of severe constraints on the data. First, the set of line integrals shall represent a systematic sampling of the entire object. If the circle of reconstruction is inscribed in an M by M image matrix, this implies $(\pi/4) \times M^2$ unknowns and a need for at least $(\pi/4) \times M^2$ linearly independent measurements. References [43], [53], [78], have examined the minimum number of views and samples per view necessary to reconstruct an arbitrary object from data in which the dominant source of noise is photon statistics. Since the presence of random noise corrupts the data, one would expect the minimum sampling requirements to be greater than they are for noise-free data as well as to be sensitive to the algorithm employed. Surprisingly, most algorithms in use today can provide stable, high-quality reconstructions for data sets approaching the theoretical minimum sampling requirements. Typically, data set sizes are on the order of one to three times the minimal amount, depending on the system and the application. Arbitrarily complex objects require more data than objects with simple geometrical shapes or highly developed symmetries.

The number of views and samples needed depends on the approach used and the amount of data required. However, independent of approach, the number of samples per view is generally more important than the number of views, and the relative proportion of views and samples should reflect this principle. Predicting the amount of noise in a CT image reconstructed with an adequate number of samples and views is a well-studied problem [25], [43], [53], [78]; predicting the amount of noise when an insufficient number of samples or views, or both, is used is more difficult and less well studied [43], [74].

Each line integral shall be accurately known. It has been found that errors in the measurement of the fractional transmittance of even a few tenths of one percent are significant [44]. This places strict requirements on the data acquisition system. As a result, the radiation detectors used in standard X-ray CT systems, along with their associated electronics, represent some of the most sophisticated X-ray sensor technology developed to date. CT systems can handle a dynamic range (the ratio of peak signal-strength-to-rms noise) as great as million-to-one [19], [33], with a linearity of better than 0,5 % [33], [64].

Each sample shall be referenced accurately to a known coordinate system. It is useless to have high precision transmission measurements if the exact ray path through the object to which it corresponds is unknown. This places strict demands on the mechanical equipment. Studies have shown that the angle of each view shall be known to within a few hundredths of a degree, and the linear position of each sample within a given projection shall be known to within a few tens of micrometres [44].

CT equipment has evolved to the stage at which each of these performance requirements can be reasonably well satisfied. A state-of-the-art scanner routinely collects millions of measurements per scan, with each one quantified accurately and referenced precisely to a specific line-of-sight through the object of interest. Once collected, the data are then passed to the reconstruction algorithm for processing.

6.5 Physical limitations on the sampling process

The quality of the reconstructed image depends on the quality of the data generated by the scanner. In actual practice, equipment and methods are limited in their ability to accurately estimate line integrals of the attenuation through an object [41]. Some of the more prominent sources of inaccuracy are the following: photon statistics, beam hardening, finite width of the X-ray pencil beams, scattered radiation, and electronic and hardware nonlinearities or instabilities, or both. Considerable attention is devoted to managing these problems.

The penetrating radiation used by CT systems is produced in a number of ways, all of which involve random atomic or subatomic processes, or both. The probability of any one atom participating at any given moment is remote, but the sheer number of atoms typically involved guarantees a finite emission rate. The number of photons produced per unit time varies because of the statistical nature of the radiation emission process. The variations have well-defined characteristics, which can be described by what are referred to mathematically as Poisson statistics. This ubiquitous radiographic problem of photon statistics is handled in CT by integrating (or counting) long enough to keep statistical noise to a diagnostically acceptable level [30], [74]. What constitutes an acceptable noise level is defined by the application and can vary widely.

Beam hardening is a problem encountered with polychromatic X-ray sources, such as X-ray tubes or linear accelerators (linacs). Such Bremsstrahlung sources, as opposed to monoenergetic (i.e., isotopic) sources, produce a flux whose average radiation energy becomes progressively higher as it propagates through an object because the lower-energy photons are preferentially absorbed with respect to the more energetic ones. This effect

compromises the validity of equation (4) since μ is no longer associated with a single energy but rather with an effective energy that is constantly changing along the ray path. Although this effect can be partially controlled by conscious engineering choices, it is generally a significant problem and shall be corrected for at some stage in the reconstructive processing (see [2], [11], [34] and references therein).

Another source of difficulties is with the finite width of the individual pencil beams. A pencil beam of X rays is geometrically defined by the size of the focal spot of the X-ray source and the active area of each detector element. Because these are finite, each source detector line-of-sight defines a thin strip rather than an infinitely thin mathematical line. As a result, each measurement represents a convolution of the desired line integral with the profile of the pencil beam. In general, the width of the strip integrals is small enough that although some loss of spatial information occurs, no distracting artifacts are generated. The exception occurs when there are sharp changes in signal level. The error then becomes significant enough to produce artifacts in the reconstructed image which manifest themselves in the form of streaks between high-contrast edges in the image. These edge artifacts [7], [41], [45], [83], are caused by the mathematical fact that the logarithm of the line integral convolved with the profile of the pencil beam (which is what is measured) does not equal the convolution of the beam profile with the logarithm of the line integral (which is what the reconstruction process desires).

Unfortunately, edge artifacts cannot be eliminated by simply reducing the effective size of the focal spot or the detector apertures, or both, through judicious collimation. As the strip integrals are reduced to better approximate line integrals and reduce susceptibility to edge artifacts, count rates become severely curtailed, which leads to either much noisier images or much longer scan times, or both. In practice, the pencil beams are engineered to be as small as practicable, and if further reductions in edge-artifact content are required, these are handled in software. However, software corrections entail some type of deconvolution procedure to correct for the beam profile [7], [41], [45], [83], and are complicated by the fact that the intensity profile of the pencil beam has a complex geometrical shape that varies along the path of the X-rays.

The same problem occurs when the structure of the object undergoing inspection changes rapidly in the direction normal to the plane of the scan. When the change is sizeable over the thickness of the slice, the same mathematics that lead to the edge artifact produce what in this case is commonly referred to as a partial-volume artifact [7], [41], [45], [83]. It manifests itself as an apparent reduction in attenuation coefficient in those parts of the image where the transverse structure is changing rapidly. In the absence of *a priori* information, nothing is known about the spatial variation of object structure within the plane of the scan, and software corrections are much more difficult to implement.

Still another source of problems arises from the presence of scattered radiation. When multiple detector elements are used, there is always the chance that radiation removed from the incident flux by Compton interactions will be registered in another detector. This scattered radiation, which becomes more severe with higher energies, cannot be easily distinguished from the true signal and corrupts the measurements. This problem can be reduced [80], but not eliminated, through the use of proper collimation.

The last type of inaccuracy is electronic and mechanical nonlinearities and instabilities. These may result from corrigible engineering deficiencies or basic physical limitations of the available components. The validity of the data is compromised in either case. In some cases, the problem can be corrected (or reduced) in software; in others, it can be fixed only by reengineering the offending subsystem. Because the bulk of existing information on this crucial topic is commercially sensitive and therefore proprietary, the literature is relatively sparse. All that can be said on these issues here is that considerable effort is required to keep these types of errors small compared to other less manageable sources of error, such as those discussed above.

6.6 Inverting the Radon transform

The reconstruction task can be defined as follows: given a set of systematic transmission measurements corrupted by various known and unknown sources of error, determine the best estimate of the cross-section of the object associated with that data. Cormack [16] and, earlier, Radon [65] showed that it is possible to “find a real function in a finite region of a plane given its line integrals along all straight lines intersecting the region”. Cormack later extended this result in a companion paper [17] that described “a method for determining a variable gamma-ray absorption coefficient in a sample from [a finite set of] measurements made outside the sample.” Although Cormack's algorithm never lent itself well to digital processing, at the time it provided a valuable existence theorem.

It was possible to recover a useful estimate of the internal structure of an object from a finite number of measurements of the X-ray transmission through an object of interest.

Over time, a large number of methods (i.e., algorithms) for recovering an estimate of the cross-section of an object (i.e., reconstructing a CT image) from its Radon transform (i.e., the set of measurements of the fractional transmittance) have evolved. They can be grouped broadly into three classes of algorithms:

a) matrix inversion methods;

b) finite series-expansion methods;

c) transform methods.

The general features of each are described below.

Matrix inversion methods follow naturally from a very direct approach to the problem of reconstructing an M by M image matrix. At the outset, an M by M matrix consists of a blank matrix of M^2 unknown attenuation values; while, on the other hand, each measurement can be described in terms of a linear combination of some fraction of these unknown attenuation values. Thus, from elementary algebraic considerations, a set of M^2 linearly independent measurements can in principle be solved for the unknown attenuation values. Further, because a set of linear equations can be solved very generally using matrices, one class of algorithms focuses on matrix methods [14].

Unfortunately, solving for N unknowns using matrices involves determining and inverting an N by N matrix. If N is a large number, such as M^2, the size of the matrix and the inversion task becomes completely intractable with current computer technology. This is not to say that matrix inversion methods are not valuable, but that they should not be judged on the basis of contemporary commercial merits. Basic research in this area is an ongoing enterprise and provides valuable insight into CT problems [43]. However, such methods shall await the further evolution of computer technology to make their way into commercial CT systems.

When the first CT instruments were introduced in the early 1970s, reconstructions were performed with what are now classified as finite series-expansion algorithms. The original EMI scanner invented by G. N. Hounsfield used such an approach [40]. These methods, which included so-called algebraic reconstruction techniques [24], simultaneous iterative reconstruction techniques [35], [37] and maximum entropy algorithms [3], [57], are rooted in a completely different branch of mathematics from the transform methods described next. Stated simply, these methods iteratively alter the reconstruction matrix until a grid of values is obtained which produces line integrals that match the measured data as nearly as possible. Obviously, a large number of figures of merit can be used to determine what constitutes the best match, given the statistical fluctuations in the data; in addition, great latitude exists in the implementation of the iterative procedure (see [14] and references therein).

While commercial CT systems no longer use iterative methods because of their inherent slowness, they offer numerous advantages that suggest they could experience a rebirth of popularity as computer technology continues to develop: e.g. they can be adapted readily to a far broader range of physical modalities and geometries (see, for instance, [81], [73]), they are reported to be less susceptible to edge artifacts [5], they are the preferred method for handling the complex reconstruction problems of emission CT [28], [32], [60], they are the best way of dealing with limited-angle data [57] or underdetermined data (too few views or samples) [52], [63], and they can be used when full three-dimensional reconstructions are performed [69], [72], as opposed to merely stacking adjacent slices. See the review article by Censor [14] for further information.

Transform methods, the third class of restorative algorithms, are based on analytical inversion formulae. Because they are easy to implement, are fast in comparison to the other methods and can produce high-quality images, they are universally used by commercial CT systems. The two primary types of transform methods are the convolution-backprojection algorithm [10], [36], [66] and the direct Fourier algorithm [65], [79], but the so-called ρ-filtered layergram method has also been used in special situations [6]. They are based on the underlying fact that the one-dimensional Fourier transform of a CT projection of an object corresponds to a spoke in Fourier space of the two-dimensional transform of that object (the so-called Central-Section Theorem or Projection-Slice Theorem [51]). Thus, in theory, all that is required in order to obtain an image by this method is to transform each projection as it is collected; place it along its proper spoke in two-dimensional Fourier space and when all the views have been processed, take the

inverse two-dimensional Fourier transform to obtain the final image. This method is called the direct Fourier transform algorithm.

Within this general framework, there is considerable latitude concerning which of the steps to conduct in Fourier space and which to conduct in direct space. The advantages of each shall be weighed against the disadvantages. The direct Fourier algorithm is potentially the faster method. However, due to interpolation problems, X-ray CT images have not yet been reported with the same quality as those obtained with the convolution-back-projection method [51], [54], [79]. Although some recent work has showed promising results [21], direct Fourier techniques are used primarily in applications that collect Fourier transforms of the projections directly, such as radio astronomy and magnetic resonance (MR) imaging [8], [39]. The convolution-back projection method (or its twin, the filtered-back projection method) is theoretically not as fast as the direct Fourier method, but it produces excellent images and with special-purpose hardware is capable of acceptable reconstruction times. The ρ-filtered layergram is impracticable when dealing with large amounts of digital data (a deficiency that obviates its use in commercial CT systems) but has the virtue of lending itself nicely to optical implementation [27], [71], a technique that could someday be used to process most CT data. These methods are reviewed, along with several tutorials, in the article by Lewitt [51].

For the sake of completeness, it should be mentioned that there is also a small class of reconstruction algorithms that are a hybrid of transform and series-expansion methods and hence do not fit logically into either of these two broad groups. Some examples are described in [51].

6.7 Convolution back-projection methods

In order to give the user a more intuitive feeling for the reconstruction process, the convolution-back-projection algorithm is described. It is provided to give a sense of how such large amounts of data can be processed efficiently into a high quality image. No effort is made to be mathematically rigorous; the interested reader is referred to [55] for a particularly readable account and to [51] for a more detailed, but still lucid, treatment of this algorithm.

First, consider the sequence of steps shown in Figure 9. Part a) shows a point object being scanned and the idealized response of a single detector as it traverses the field of view. Part b) shows each of the many profiles collected during this scan back-projected across an initially blank circle of reconstruction. Back-projection can be thought of as reversing the data collection process. Each sample within a given projection represents the fractional transmittance of a narrow beam of X-rays through the object, which is assumed to be sufficiently well approximated by small, discrete pixels of constant attenuation. During back-projection, the value of each sample in the profile is numerically added to all of the image pixels that participated in the attenuation process for that sample. Conceptually, back-projection can be thought of as smearing each profile back across the image in the direction of the radiation propagation.

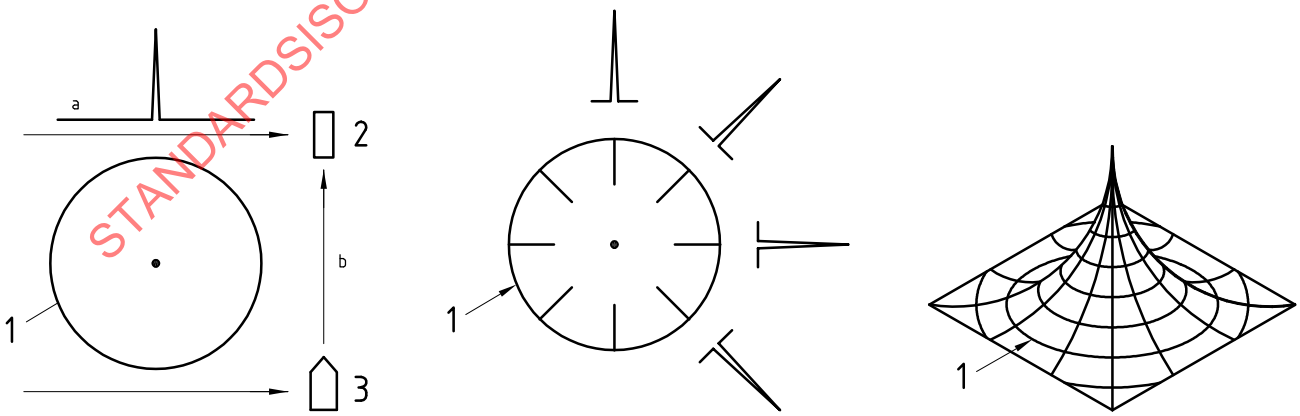

a) Projection of a point object **b) Normal back projection technique** **c) Reconstructed image of a point**

Key

1 Circle of reconstruction
2 Detector
3 X-ray source
a Detector response.
b X-rays.

Figure 9 — Straight back-projection

Part c) shows the net result of this operation. For a point object, the profiles superimpose to produce a central spike with a broad skirt that falls off as $1/r$ (at any radius, the number of back-projected rays radiating from the centre is a constant). It is implicitly assumed here that a large number of profiles have been used; hence the smooth, featureless falloff. One of the earliest attempts at reconstruction used this approach [62]. The product was a blurry but diagnostically useful image, at least in the absence, at that time, of a viable alternative.

Figure 10 shows an improved version of this basic approach. Part a) shows the same scan situation as depicted in Figure 9. In part b) however, each profile has been convolved with a function that preserves the essential response of the detector to the presence of the point object but adds a negative tail to beat down the $1/r$ falloff that occurs with pure back-projection. The result of back-projecting these modified profiles is schematically illustrated in part c) where the point object is shown reconstructed in much sharper detail. This so-called convolution-back-projection method is the method used by virtually all commercial CT systems. It is easy to implement with digital techniques, is numerically robust and is adaptable to special-purpose computer equipment, such as array processors or hardwired back-projectors.

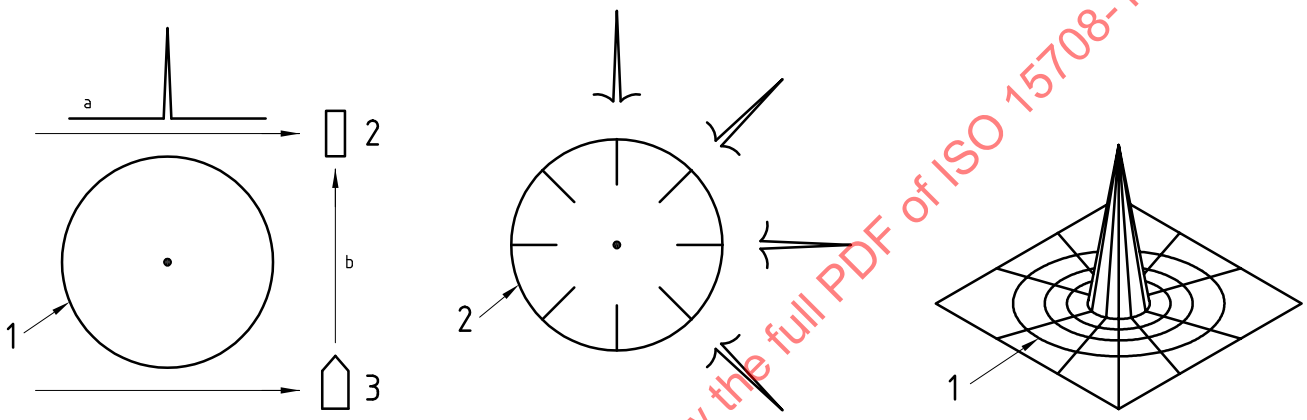

a) Projection of point object **b) Filtered back projection technique** **c) Reconstruction image of a point**

Key

1 Circle of reconstruction
2 Detector
3 X-ray source

a Detector response.
b X-rays.

Figure 10 — Convolution back-projection

To obtain an idea of how this appears mathematically, the results of equation 4 are rewritten in the following form:

$$P(\theta,\rho) = -\ln[I(\theta,\rho)/I_0] = \int \mu(x,y)ds \tag{5}$$

As before, I represents a single ideal measurement, but it has been rewritten to explicitly recognize that the detector is oriented with respect to the object at some angle, θ, and some position, ρ, as indicated in Figure 8. I_0 is the unattenuated signal level, $\mu(x, y)$ is the two-dimensional distribution of the linear attenuation coefficient of the object, and ds is an element of distance along the X-ray path through the object at angle θ and position ρ. The values of $I(\theta, \rho)$ are normalized to unity and logged to yield a set of estimated line integrals through the object, $P(\theta, \rho)$.

With this notation, the convolution-back projection process schematically shown in Figure 10 can be written as follows:

$$\mu(x,y) = \int_0^{\pi}\int_{-\infty}^{\infty} P(\theta,\rho)\times g(\rho-\eta)\times d\eta\times d\theta \tag{6}$$

where g is the convolution function of the shape-theoretical form:

$$g = \frac{\pi^2}{2}\left(\frac{\delta(r)}{r} - \frac{1}{r^2}\right) \tag{7}$$

in which $\delta(r)$ is the Dirac delta function.

There is an obvious problem with expressing $g(r)$ in this form when working with digital computers. A severe discontinuity exists near the origin where, loosely speaking, the delta function must in some way be attached to the $-1/r^2$ tail. However, this expression is presented only to give the reader an idea of the behaviour of $g(r)$. The rigorous mathematics of how such functions are handled digitally in practice are treated in the literature (see [51] and [55] and references therein).

In words, equations (6) and (7) say that $\mu(x, y)$ can be recovered from a complete set of line integrals, $P(\theta, \rho)$, by first convolving each projection with a special function, g [i.e., the integral over η in equation (6)] and then back-projecting each convolved view to obtain the final image [i.e., the integral over θ in equation (6)]. Convolving the views with the function, g, given in equation (7) accomplishes two tasks: i) the first term is just the polar-coordinate version of the delta function and serves to preserve the basic profile of each view; and ii) the second term corrects for the blurring introduced by the back-projection algorithm. In CT terminology, if the convolution is conducted in direct space (i.e., the inner integral in equation (6) is evaluated directly), the method is called convolution back-projection. If it is conducted in Fourier space (which is generally a much faster way to do it), the method is called filtered back-projection. This distinction is frequently overlooked, and the two terms are often used interchangeably.

7 Interpretation of results

7.1 Technical Objectives

The goal of a CT X-ray imaging system is to non-destructively produce internal images of objects with sufficient detail to detect crucial features. The task of the CT user is to specify the system that will satisfy a particular need and to verify that the specification is met. The visibility of a feature in a CT image depends on the difference in X-ray attenuation between the feature and its background, size of the feature, size of the background object, X-ray optics, number of samples collected, X-ray exposure and numerous other factors. To accurately predict the performance of a given system in specific application requires a very complicated modelling process. However, many researchers have shown that detectability obeys some fairly simple rules and can be expressed as a function of system noise, system resolution, size and composition of the background object, and size and composition of the feature.

It is shown in 7.2 to 7.7 how these rules can be used to help specify a CT system as well as how they can be used to verify a specification. Background is presented to help the user understand the roles of CT system resolution and noise in detectability. Contrast is defined in 7.2. The effect of system resolution on contrast is discussed in 7.3. The effect of system noise on contrast is discussed in 7.4. The findings of various researchers that relate contrast detectability (with a 50 % confidence level) to object size and system noise are presented in 7.5. These aspects are combined in 7.6 to aid the user in specifying a system for a particular need. The user is shown how to measure the performance of an existing system in 7.7.

7.2 Contrast

The quantity that is reconstructed in X-ray CT imaging is the linear attenuation coefficient, μ, usually within a two-dimensional slice defined by the thickness of the X-ray beam. It is measured in units of cm^{-1} and is directly proportional to the electron density of the material. To be distinguishable, a feature shall have a linear attenuation coefficient, μ_f, that is sufficiently different from the linear attenuation coefficient of its background material, μ_b.

Linear attenuation coefficients are functions of the incident X-ray energy, E. Figure 11 shows the functional energy dependence of the X-ray linear attenuation coefficients of two hypothetical materials, μ_f and μ_b. It is seen that the degree of contrast, $\Delta\mu$, between two materials varies greatly as a function of the energy. (For simplicity in these discussions, the X-rays used are assumed to have a single energy, E, or to be approximated by some mean energy, $\overline{E}$, if a spectrum of energie is used.) The X-ray energy is an important parameter that shall be chosen for a given scan specification. It would seem advantageous to choose a low energy to maximize contrast; however, the

attenuation coefficient is large for low energies, and this results in poor X-ray transmission and high system noise, which is detrimental to good detectability. Also, higher-energy systems usually have significantly higher X-ray flux than lower energy systems. The optimum trade-off clearly depends, to a great extent, on the specific application.

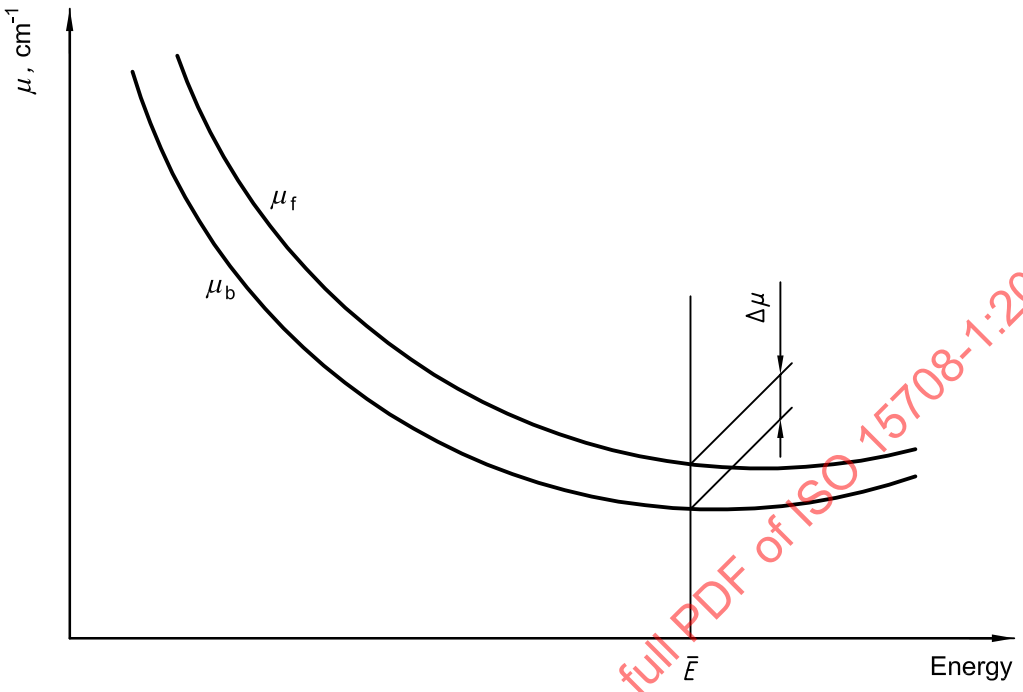

Figure 11 — Difference $\Delta\mu$ upon the energy of incident X-rays

Contrast in CT has been defined historically as the percent difference of a feature from a background material.

$$\text{Contrast in \%} = \frac{|\mu_f - \mu_b|}{\mu_b} \times 100 \tag{8}$$

This expression has the disadvantage of being infinite for a feature in air, for which μ_b is effectively zero, but it is convenient for comparing the contrast of different materials in a given background. It should be noted that this definition for contrast assumes that the feature in question extends throughout the thickness of the CT slice. If the feature has thickness h but is imaged with a slice of larger thickness t, the contrast is further reduced by the factor h/t.

If the CT imaging system did not introduce degradation, a profile through the centre of the feature shown in Figure 12 a) would have the crisp shape shown in Figure 12 b). Probability-distribution functions PDF(μ_f) and PDF(μ_b), which describe the probabilities of finding a given value μ inside the feature and inside the background, respectively, are plotted in Figure 12 c). In the absence of degradation, only the value μ_b appears in the background, and only the value μ_f appears in the feature, with each normalized to unit probability. The contrast difference, $\Delta\mu$, is simply given by:

$$\Delta\mu = |\mu_f - \mu_b| \tag{9}$$

As resolution and noise are introduced into the discussion, the effect of each on the profile of Figure 12 b) and the PDF of Figure 12 c) will be monitored.

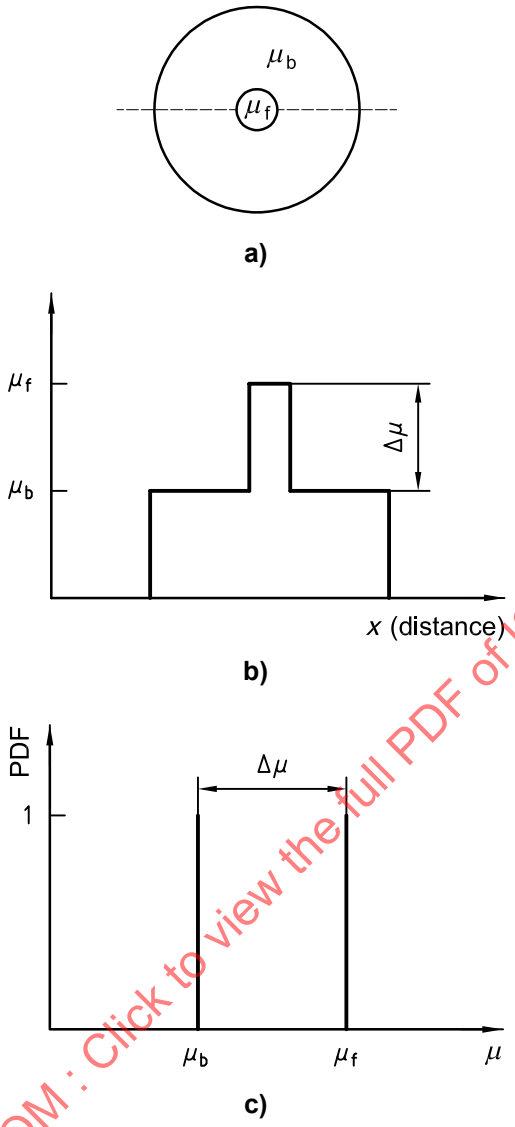

Figure 12 — a) Sketch illustrating a CT reconstruction of a small feature of attenuation coefficient μ_f embedded in the centre of a background material of attenuation coefficient μ_b; b) plot of the CT density profile through the feature in a); c) probability distribution function (PDF) for the attenuation coefficients found in a)

7.3 Resolution

The finite number and width of the X-ray beams cause the blurring of a feature, which can alter both the shape of the feature and the resolvability of multiple features. This blurring also affects the perceived contrast, especially of small features. To a first approximation, it is possible to derive a two-dimensional blurring function that can be convolved with an object to produce the equivalent of a CT image. This blurring function, called the point-spread function (PSF), is the response of the system to an ideal point object. In this discussion, it will be assumed that the PSF has circular symmetry and is uniform throughout the image. In this case, the modulus of the one-dimensional Fourier transform of a profile through the PSF gives the modulation transfer function (MTF)[23] of the system, which describes the differential ability of the system to reproduce spatial frequencies. In general, low frequencies (large, homogeneous features) are reproduced more faithfully than high frequencies (small features).

First, a simple approximation to the PSF is discussed, and its effect on the profile of Figure 12 b), on the PDF of Figure 12 c), and on the effective contrast of small features is illustrated. Three methods of obtaining the MTF are then discussed: one theoretical and two experimental. It should be emphasized that the MTF is not merely a computational curiosity; it is used both to predict and to measure system performance.

For the purpose of illustration, the PSF can be approximated by a cylinder of diameter BW[83] that approximates the beam width. BW is a function of the detector width d, the X-ray source width a, the distance between the source and the detector L, and the distance between the source and the imaging point q as follows:

$$BW \cong \frac{\sqrt{d^2 + \left[a(M-1)\right]^2}}{M} \tag{10}$$

where $M = \frac{L}{q}$ (11)

The quantities d, a, L and q are illustrated in Figure 13. A justification for equation 10 will be given in the discussion of the MTF that follows (see also [83]).

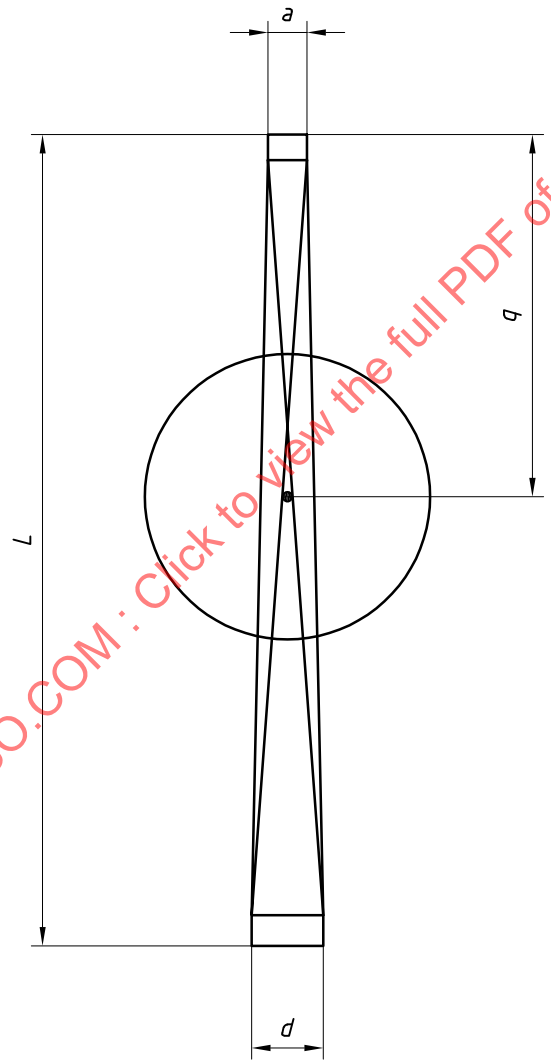

Figure 13 — Sketch illustrating the geometry of the X-ray beam of a CT scanner, where d is the detector width, a is the X-ray source width, L is the distance between the source and the detector and q is the distance between the source and the imaging point

Figure 14 shows the convolution of the PSF with features that are smaller than, equal to, and greater than the PSF. Figure 4 a) shows the result of convolving the PSF of diameter BW with a smaller feature of diameter SW and contrast difference $\Delta\mu$. The imaged feature will be a truncated cone with base ($BW + SW$) and contrast difference $\Delta\mu(SW/BW)^2$ Thus, the system PSF reduces the contrast of features smaller than the beam width by the ratio of

their areas and increases the width of the imaged feature to approximately that of the PSF. Figure 14 b) shows the result of convolving the PSF of diameter BW with a feature of diameter BW and contrast $\Delta\mu$. The imaged feature will be a cone of base $2BW$ and maximum contrast difference $\Delta\mu$. Figure 14 c) shows the result of convolving the PSF of diameter BW with a larger feature of diameter LW and contrast difference $\Delta\mu$. The imaged feature will be a truncated cone of base $(BW + LW)$ and contrast difference $\Delta\mu$. Thus, the diameters of features much wider than the PSF are affected only slightly, and the contrast in their centres is not altered. These results will prove very useful later in the discussion on the relationship between detectability and feature size.

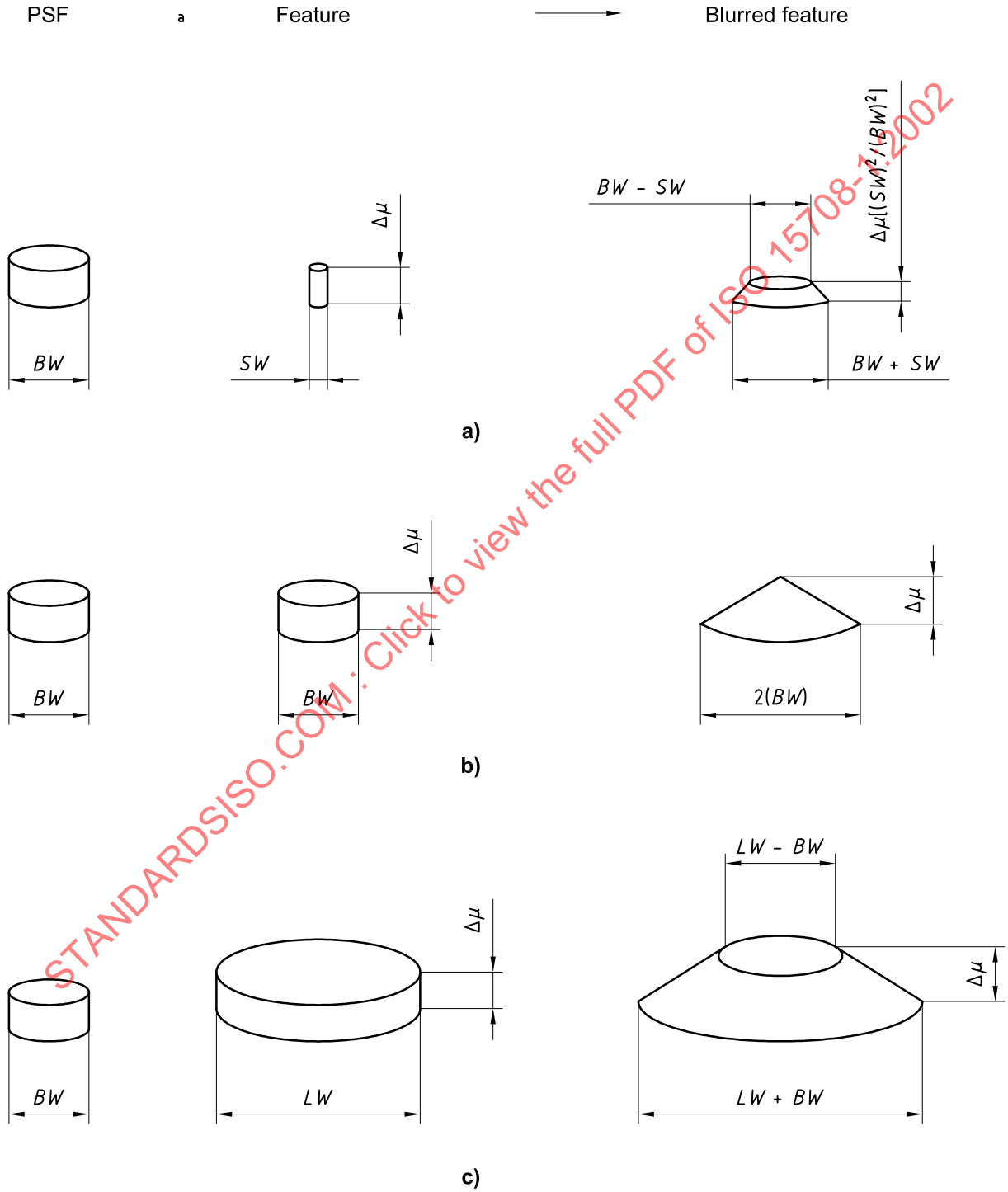

a Convolution of two functions.

Figure 14 — Sketch illustrating the two-dimensional convolution of a point-spread function (PSF) of diameter BW with features of varying diameters: a) $SW < BW$; b) $BW = BW$; c) $LW > BW$

The fact that the CT imaging process is discrete rather than continuous has been ignored thus far. In fact, the projection data is sampled at some discrete spatial increment, s. Sampling theory dictates that s be $BW/2$ at the most. The presentation of the reconstructed image is also discrete. Again, sampling theory holds that pixel size, Δp, in the reconstructed image shall be equal to or smaller than s in order to preserve spatial resolution. In terms of the convolution of Figure 14, the smallest feature will occupy at least four (2^2) pixels, and possibly more.

Figure 15 a) shows the effects on image fidelity that convolution with the PSF and discrete sampling has had on the ideal image of Figure 12 a). The profile through the feature is now rounded at the edges. Figure 15 b), which is a plot of the new probability-distribution functions (PDFs), shows that the PDF of the background now has values larger than μ_b and that the PDF of the feature has values smaller than μ_f.

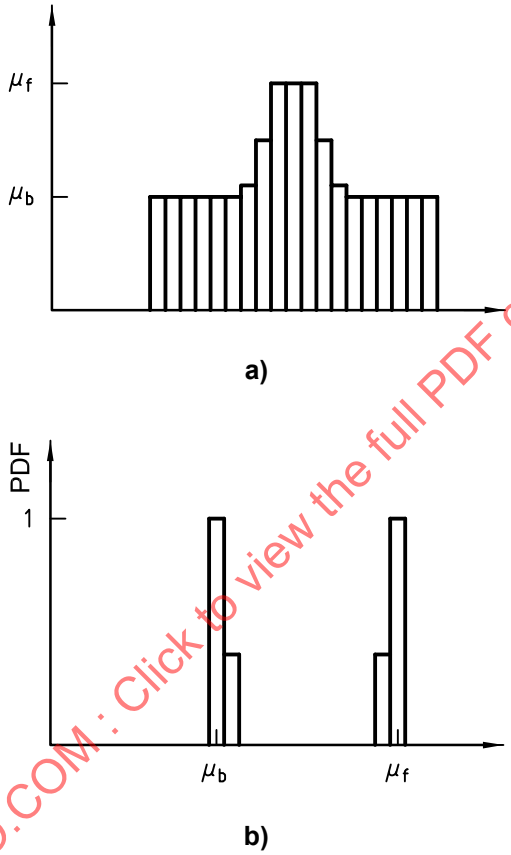

Figure 15 — a) One-dimensional profile through the centre of a feature convolved with a CT PSF and pixelized; b) a probability-distribution function for the profile in a)

The convolution of multiple features in the image with the PSF of the system illustrates the concept of the modulation-transfer function (MTF). Figure 16 shows a central, one-dimensional profile of the convolution of the PSF of width BW with periodic features of diameter D whose centres are separated by $2D$. These periodic features are dominated by spatial frequencies of value $1/(2D)$. Notice that as long as $D \geqslant BW$, the effective contrast $(\Delta\mu)_e$ is not reduced; whereas for $D < BW$, the effective contrast is reduced. Furthermore, there is no contrast at all at approximately $D = BW/2$. This spatial frequency at approximately $1/BW$ is called the cut-off frequency and represents the effective resolution limit of the system because frequencies above this value are significantly altered by the system and cannot contribute to a faithful representation of the object. Figure 17 d) shows a plot of the ratio of the effective contrast, $(\Delta\mu)_e$, to the true contrast, $\Delta\mu$, as a function of the spatial frequency $1/(2D)$. This is the MTF curve. It can be measured experimentally for a real system from scans of spatial gages similar to those of Figure 16. However, this method is open to interpretation and is not recommended for an impartial system analysis.

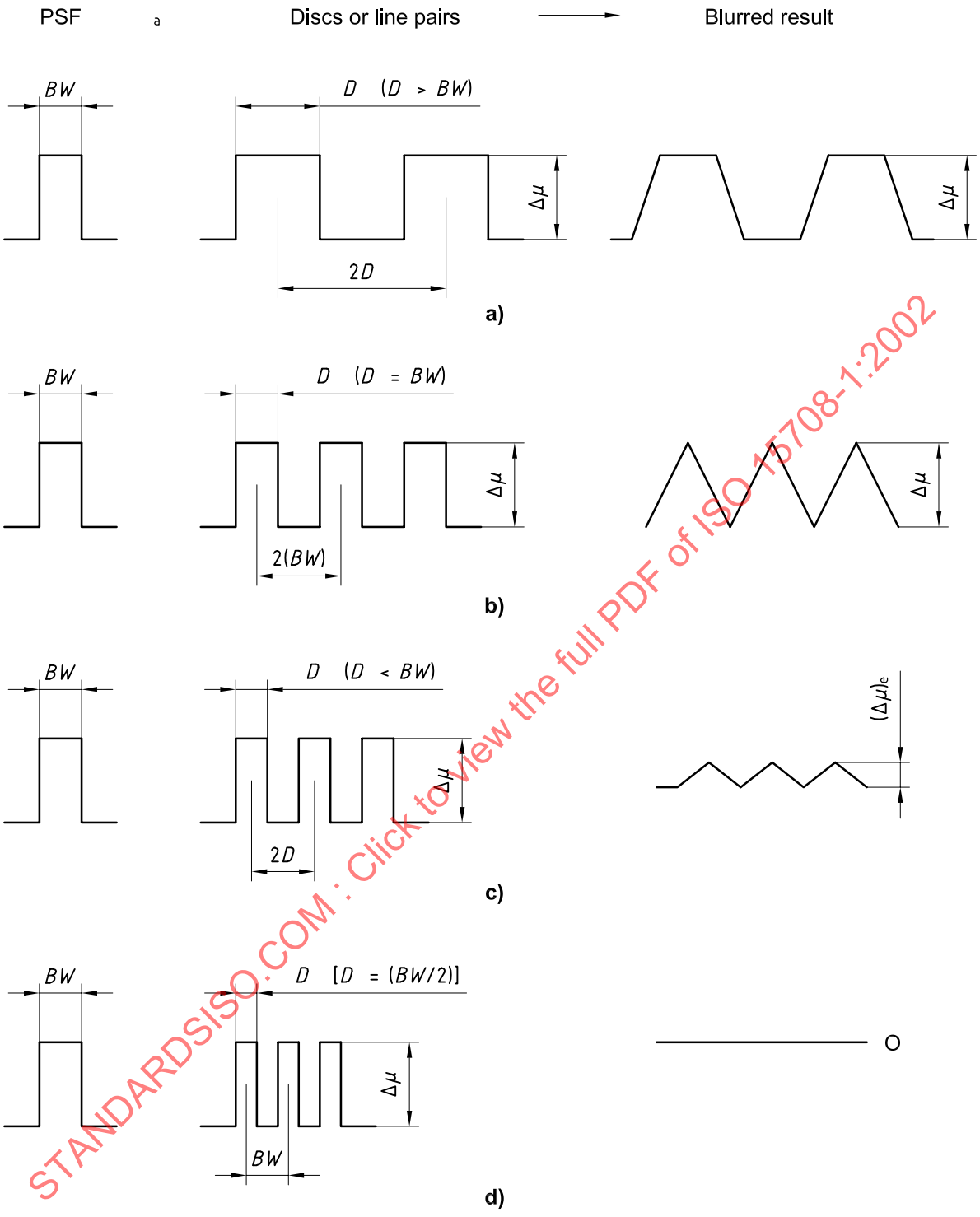

a Convolution of two functions.

Figure 16 — Illustration of a one-dimensional profile through the centre of periodic features of varying diameters which have been convolved with a CT PSF: a) $D > BW$**; b)** $D = BW$ **c)** $BW/2 < D < BW$**; d)** $D = BW/2$

The following discussion describes how to obtain a theoretical expression for the MTF of a hypothetical system. The formalium applies to a parallel-beam method of data collection, but the expressions for fan-beam data collection are analogous. The method is attributed to Glover and Eisner [23], who show that the MTF is approximately equal to the one-dimensional Fourier transform (FT) of a circularly symmetric PSF and is given by the following expression:

$$\mathrm{MTF}(f) = \frac{F_{\mathrm{CON}}(f)}{f} \times F_{\mathrm{BW}}(f) \times F_{\mathrm{MOV}}(f) \times F_{\mathrm{INT}}(f) \times F_{\mathrm{PIX}}(f) \tag{12}$$

where:

f is the spatial frequency variable;

$F_{\mathrm{CON}}(f)$ is the FT of the convolution function;

$F_{\mathrm{BW}}(f)$ is the FT of the effective beam width;

$F_{\mathrm{MOV}}(f)$ is the FT of the data integration factor;

$F_{\mathrm{INT}}(f)$ is the FT of the linear interpolation function in the image reconstruction;

$F_{\mathrm{PIX}}(f)$ is the FT of the display function.

The factor $F_{\mathrm{CON}}(f)/f$ is the convolution filter factor, assuming a reconstruction process of parallel-beam convolution and back-projection. (The reconstruction process is beyond the scope of the present discussion.) The interested reader is referred to Ramachandran [66] or Shepp and Logan [76]. The filter factor due to Ramachandran is used when high resolution is desired and the contrast is large enough that noise is not an issue. The filter factor due to Shepp and Logan is used when noise is high, contrast is low and high resolution is not the primary objective. The factors for these two filters are given below, where s is the linear spacing between samples in a profile:

$$\frac{F^{\mathrm{R}}_{\mathrm{CON}}(f)}{f} = 1 \text{ [Ramachandran]} \tag{13a}$$

$$\frac{F^{\mathrm{S\&L}}_{\mathrm{CON}}(f)}{f} = \frac{\sin(\pi f s)}{\pi f s} \text{ [Shepp and Logan]} \tag{13b}$$

Yester and Barnes [83] describe the FT of an arbitrary beam shape as follows, where these quantities are defined in equations 10 and 11:

$$F_{\mathrm{BW}(F)} = \frac{\sin\left[\frac{\pi f d}{M}\right]}{\frac{\pi f d}{M}} \times \frac{\sin\left[\frac{\pi f a (M-1)}{M}\right]}{\frac{\pi f a (M-1)}{M}} \tag{14}$$

They also note that this function can be approximated to a good approximation by the FT of a square beam whose width is BW, given previously by equation (10).

Collecting discrete signals from a moving X-ray source is equivalent to convolution by a square function whose width is the linear sampling increment s. Its FT is given by the following:

$$F_{\mathrm{MOV}(f)} = \frac{\sin(\pi f s)}{\pi f s} \tag{15}$$

Since data values are computed at discrete points and the reconstruction process requires values at intermediate points, some form of interpolation shall be conducted. One common form is linear interpolation whose FT has the following form:

$$F_{\mathrm{INT}} = \frac{\sin^2(\pi f s)}{(\mu f s)^2} \tag{16}$$

Finally, the interpolated data are displayed on a square grid of width Δ_ρ. Since this representation is equivalent to a convolution, the MTF is also multiplied by the following factor:

$$F_{\mathrm{PIX}} = \frac{\sin(\pi f \Delta p)}{\pi f \Delta p} \tag{17}$$

Equation 12 is useful for predicting the MTF of a hypothetical system. The relationship between the PSF and the MTF also suggests a superior method for measuring the MTF of an existing system. Since the PSF is ideally the system response to a point function, a point can be imaged, and the PSF can be obtained directly as a profile of this point image. In practice however, point objects always have some width. Fortunately, it can be shown that the one-dimensional profile of a circularly symmetric PSF is roughly equivalent to a profile taken perpendicular to the two-dimensional response of the system to a line, the line-spread function (LSF)[46]. Although a line is equally difficult to image, the LSF is well approximated by the first derivative of the response of the system to an edge, the so-called edge-response function (ERF), which is obtained easily.

Figure 17 illustrates the process of obtaining the MTF experimentally from the image of a simple cylinder. The use of a cylinder [Figure 17 a)] is preferred because, once its centre of mass is determined, profiles through this point are perpendicular to the cylinder edge. Many profiles can be aligned and averaged to reduce system and quantization noise on the edge-response function (ERF) [Figure 17 b)]. The LSF is estimated by taking the discrete derivative of the ERF [Figure 17 c)], and its discrete FT is taken to obtain the MTF [Figure 17 d)]. This procedure is easy to execute and not open to misinterpretation.

NOTE By convention, the height of the MTF is normalized to unity.

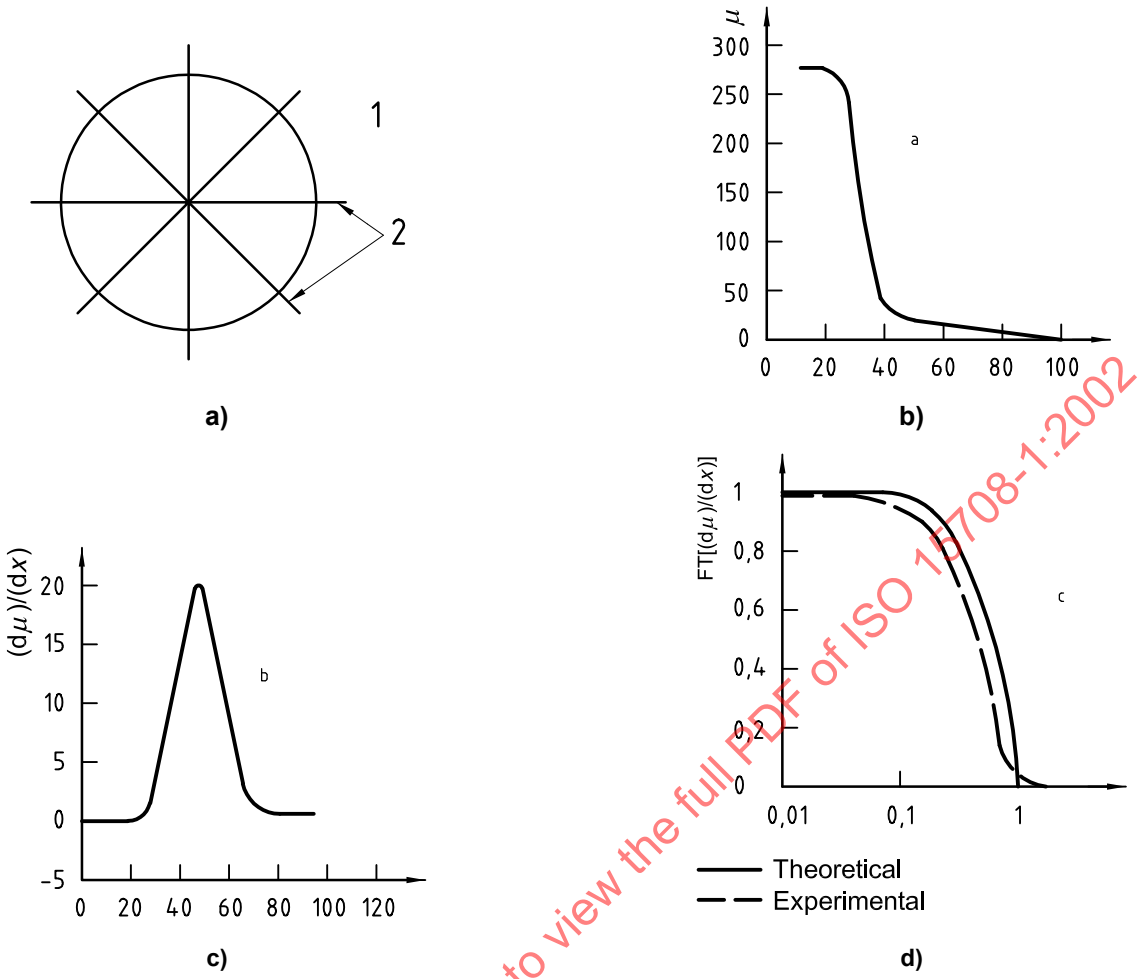

Key

1 Imaged cylinder
2 Edge profiles

a Edge response function (ERF).
b Line spread function (LSF).
c MTF for Shepp/Logan filter.

Figure 17 — Illustration of the procedure for obtaining the MTF from a CT image of a small cylinder: a) sketch indicating relative orientation of three different line profiles through the centre of the imaged cylinder; b) result of aligning and averaging many edge profiles, the edge-response function, ERF; c) system line-spread function, LSF, obtained by differentiation of the ERF; d) system modulation-transfer function, MTF, obtained by discrete Fourier transformation of the LSF

7.4 Noise

In 7.3 the extent to which the system PSF degrades contrast and resolution was investigated. However, no factor has been introduced thus far that would prevent detection of a feature (except at the cut-off frequency). In this subclause, system noise is added to the model of system behaviour, and its impact on detectability is explored in terms of basic system performance parameters.

It is not possible to build an X-ray CT imager without noise. Even if electronic noise and scatter noise are minimized, quantum statistics dictate that there will be variation in the number of X-rays detected from the source. The photon noise on the X-ray signal is known to obey Poisson statistics; i.e., it is characterized by the fact that the variance of the signal is equal to its mean. It is customary to specify noise as the standard deviation, which is the

square root of the variance. This means that if an average of n photons is detected in a given sampling period, the number actually recorded in any particular interval will be in the range of $n \pm n$ approximately 70 % of the time.

The effect that noise has on a CT image is complicated by the reconstruction process. For a parallel-beam scanner geometry, Barrett and Swindell[4] show that the noise at the centre of a reconstructed cylinder of radius R_0 irradiated by X-rays of effective energy $\bar{E}$ is given by the following formulae for the Ramachandran (σ_R) and Shepp and Logan ($\sigma_{S\&L}$) convolution filters:

$$\sigma_R \cong \frac{0{,}91}{s\sqrt{V}}\sigma_d \text{ [Ramachandaran]} \tag{18a}$$

$$\sigma_{S\&L} \cong \frac{0{,}71}{s\sqrt{V}}\sigma_d \text{ [Shepp and Logan]} \tag{18b}$$

where:

s is the spatial sampling increment;

V is the number of views or orientations;

σ_d is the standard deviation of the noise on the samples in the profile data.

The computation of the noise on the profile data, σ_d, is complicated by the fact that the profile data give the natural logarithm of the ratio of the intensity of the unattenuated radiation, n, and the detected signal. Also, there is likely to be additional noise from the detector electronics and scattered radiation. In a detailed analysis, these contributions shall be included, and they will increase the noise. However, in the approximation that photon noise dominates, the minimum possible data noise, σ_d, is given by the following expression, where $\mu_o(\bar{E})$ is the linear attenuation coefficient of the cylinder:

$$\sigma_d \cong \left[\frac{1}{n\exp\left[-2\mu_0\left(\bar{E}\right)R_0\right]}+\frac{1}{n}\right]^{1/2} \tag{19}$$

Notice that the noise decreases with increasing n and increases with increasing R_o or μ_o.

Experimentally, the usual process for determining the standard deviation, σ, for a homogeneous area of a reconstructed image containing m pixels, each with some value μ_i, is to first find the mean value of the set of m pixels:

$$\bar{\mu} = \frac{1}{m}\times\sum_{i=1}^{m}\mu_i \tag{20a}$$

and then compute σ as:

$$\sigma = \left[\frac{\sum_{i=1}^{m}\left(\mu_i-\bar{\mu}\right)^2}{m-1}\right]^{1/2} \tag{20b}$$

where:

Σ is summation over the region of interest;

σ is a measure of the spread of the values of μ_i about the mean $\overline{\mu}$.

Hanson [31] shows that σ is not very sensitive to the number of pixels averaged if m is in the range of $25 \leqslant m \leqslant 100$. The noise in a reconstructed image does have a positional dependence, especially near the edges of an object, so extremely large regions shall not be used. Hanson [30] has also shown that the noise in CT images is not completely uncorrelated, but the effect on σ is small.

Figure 18 a) shows the effect that noise has on the blurred, pixelized image of Figure 15 a). The noise appears as a jitter superimposed on the profile of the feature. Figure 18 b), which shows the new PDFs, illustrates that the spread of attenuation values has increased and that the two distributions may overlap. The photon noise on any one sample is Poisson distributed, but the combination of independent samples is approximated better by the normal distribution given by the following expression:

$$\mathrm{PDF}(\mu) = \frac{1}{\sqrt{2\pi\sigma}} \times \exp\left[-\frac{\left(\mu - \overline{\mu}\right)^2}{2\sigma^2} \right] \tag{21}$$

where:

$\overline{\mu}$ is the mean of the distribution;

σ is the standard deviation.

Equation (21) has the advantage of being computationally simple. Figure 18 c) shows the PDFs redrawn as smooth curves. The figure illustrates the fact that 70 % of the values are within $\pm\,\sigma$ of the mean.

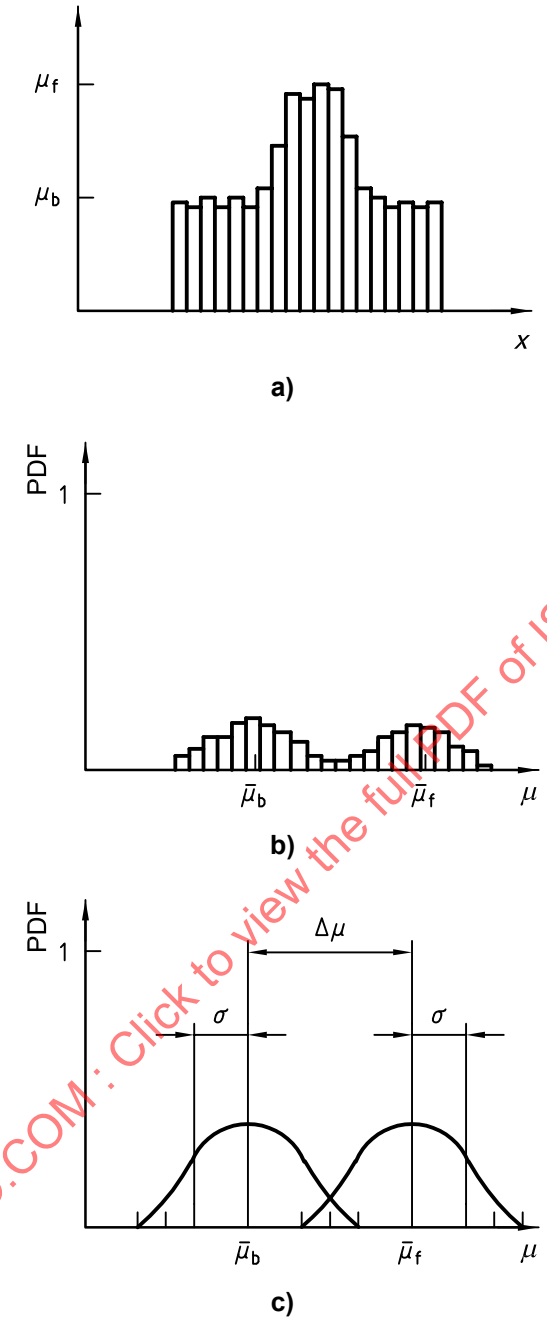

Figure 18 — a) Line profile through the centre of a noisy feature convolved with a CT PSF and pixelized: b) probability-distribution function for the profile in a); c) continuous representation of the PDFs of b) with the means, standard deviations and contrast difference indicated

Figure 18 c) shows that the contrast will be degraded. The difference in contrast can now be defined to be the difference between the mean of the feature, $\bar{\mu}_f$, and the mean of the background, $\bar{\mu}_b$. However, if a detection threshold is placed between the two distributions and they overlap, there will be instances when pixels within the feature will be counted as background and pixels within the background will be counted as features.

7.5 Contrast-Detail-Dose (CDD) curve

In practice, detection is not based solely on threshold criteria. Human beings use visual integration when detecting features, and even computer detection processes are likely to use pattern recognition techniques. Thus, detection criteria should be based on the observations of human beings. Several investigators [15], [31], [75] have reported that the effective contrast, $(\Delta\mu)_e$, which human beings can detect with a 50 % probability of success, depends on the image noise, σ, and the object diameter, D, according to the following relationship:

$$(\Delta\mu)_e \cong \frac{c\sigma\Delta p}{D} \tag{22}$$

where:

c is a constant in the range of $2 \leqslant c \leqslant 5$;

Δp is the pixel width.

It is seen from Figure 14 that the contrast difference of features larger than the effective beam width BW is not affected by beam convolution. Thus, for large features:

$$(\Delta\mu)_e = \Delta\mu \cong \frac{c\sigma\Delta p}{D}\left[D \gg BW\right] \tag{23a}$$

Dividing equation (23a) by μ_b and multiplying by 100 % gives the formula for percent contrast:

$$\frac{|\mu_f - \mu_b|}{\mu_b} \times 100 = \frac{c\sigma\Delta p}{D\mu_b} \times 100\left[D \gg BW\right] \tag{23b}$$

Equation (22) has not been tested for features smaller than BW. However, the results of Figure 14 suggest a logical extension. Features smaller than BW have effective diameter BW and have the contrast reduced by $D^2/(BW)^2$. Thus, the detectability limit for smaller features can be approximated by the following:

$$(\Delta\mu)_e = \frac{\Delta\mu D^2}{(BW)^2} \cong \frac{c\sigma\Delta p}{BW}\left[D \gg BW\right] \tag{24a}$$

and the percent contrast is given by the following:

$$\frac{|\mu_f - \mu_b|}{\mu_b} \times 100 = \frac{c\sigma BW\Delta p}{D^2\mu_b} \times 100\left[D \gg BW\right] \tag{24b}$$

Detectability alone is often not sufficient; features shall be discriminated (detected and resolved). Equation (22) can also be used to predict the discrimination of pairs of features of diameter D separated by $2D$. This distance is used because it is conventional to define resolvability in terms of the classical Rayleigh sense, which stipulates a $2D$ separation. From Figure 16, it has been shown that in this case, $(\Delta\mu)_e$ is given by the product of the true contrast times the system modulation-transfer function (MTF). In this case, the perceived contrast, $(\Delta\mu)_e$, is given by the following expression:

$$(\Delta\mu_{CDD})_e = \Delta\mu_{CDD} \times \mathrm{MTF}(1/2\,D) = \frac{c\sigma\Delta p}{D} \tag{25}$$

Solving equation (25) for $\Delta\mu_{CDD}$, dividing by μ_b, and multiplying by 100 % gives an expression for the percent contrast for threshold (50 %) discrimination:

$$\frac{|\mu_f - \mu_b|}{\mu_b} \times 100 = \frac{c\sigma\Delta p \times 100}{\mathrm{MTF}(1/2\,D)D\mu_b}\left[CDD\right] \tag{26}$$

The plot of the contrast required for 50 % discrimination of pairs of features as a function of their diameters in pixels is called a contrast-detail-dose (CDD) curve.

7.6 Performance prediction

The detectability limits defined by equations (23b) and (24b) can be used to estimate the detection ability of a proposed CT system in order to detect an object of a given size and composition. In the interest of simplicity, detectability will be computed at the centre of a uniform cylinder. The noise in a reconstructed cylinder is highest at its centre so that this represents the worst case. Also, many complex objects can be approximated by a cylinder of the same material and cross-sectional area.

The contrast given in equations (23b) and (24b) is a function of μ_b, which in turn depends on the X-ray source effective energy $\overline{E}$, the pixel size Δp, the size of the feature relative to the X-ray beam width BW and the noise σ. Many references list linear attenuation coefficients as functions of $\overline{E}$ [42], [56]. BW is defined by equation 10 and Figure 13 in terms of the source width, detector width and position of the object. For a parallel-beam CT scanner, σ is given by equations (18a) and (18b) in terms of the sampling increment s, the number of views V, the cylinder radius R_o, and the number of unattenuated photons incident in each sample n. Once these parameters are specified, it is possible to plot a detectability graph that will predict the performance of the scanner.

Figure 19 shows the detectability graph for an iron cylinder 2,54 cm in radius that is irradiated with 0,8 MeV X-rays. The detectability line for objects of diameter $D >> BW$ [equation (23b)] is represented by a solid line. For ease of analysis, the $\log_{10}$ of the percent contrast has been plotted as a function of the $\log_{10}$ of the feature diameter, D, measured in pixels. The detectability line for objects of diameter $D << BW$ [equation (24b)] is represented by a dashed line. To determine whether a feature of given diameter, D, and linear attenuation, μ_f (0,8 MeV), will be detected in the centre of this iron cylinder, plot the point whose ordinate is the percent contrast:

$$100\ \% \times |\mu_{FE}\ (0{,}8\ \text{MeV}) - \mu_f\ (0{,}8\ \text{MeV})| / \mu_{FE}\ (0{,}8\ \text{MeV})$$

and whose abscissa is the diameter D in pixels. If this point falls well to the right of the lines, it will be detected more than 50 % of the time. If it falls to the left, it will not. Remember that the percent contrast shall be multiplied by the ratio h/t if the height of the feature h is less than the X-ray slice width t.

It is also possible to plot the theoretical CDD curve specified by equation (26). The theoretical MTF has been given in equation (12) as a function of specified scanner parameters. The theoretical CDD curve for the iron cylinder is identified in Figure 20 by the short dashed curve. To determine whether two features of diameter *D* whose centers are separated by 2*D* can be discriminated at least 50 % of the time, plot a point whose ordinate is the percent contrast and whose abscissa is their common diameter in pixels. Determine the position of the point relative to the curve. If it lies well to the right of the curve, the features will be discriminated with at least a 50 % probability.

7.7 Performance verification

The detectability and CDD curves for an existing CT scanner can also be plotted from equations (23b), (24b) and (26) for a cylinder of specified material and size. The quantity σ/μ_b is the noise-to-signal ratio at the centre of the cylinder as computed from equations (20a) and (20b). The function MTF(1/2 D) is computed experimentally from a small cylinder as described in Figure 17. Figure 20 shows a comparison of the predicted (solid line) and measured (dotted line) CDD curves from an existing CT scanner for an iron cylinder 2,54 cm in radius irradiated by an equivalent energy of 0,8 MeV. A comparison between the experimental and theoretical MTF curves is shown in Figure 17 d). The agreement between the theory and experiment is quite good in this case. Because the cylinder is relatively small, there is not a large contribution to the noise from scattered radiation. For a large cylinder, scatter will usually make the experimental noise larger than the predicted noise, and the curve will shift upwards.

7.8 Conclusion

A simple formalism for the prediction and evaluation of the performance of X-ray CT systems has been presented. Contrast has been defined and the degradation of contrast by the system point-spread function and the system noise has been discussed. Finally, the use of a simple object has been recommended to predict and verify the performance of CT systems in the detection and discrimination of features in a background of specified size and

composition. It shall be emphasized that this formalism is meant to be a simple indicator of system capabilities and does not address such complications as detection in the presence of CT artifacts.

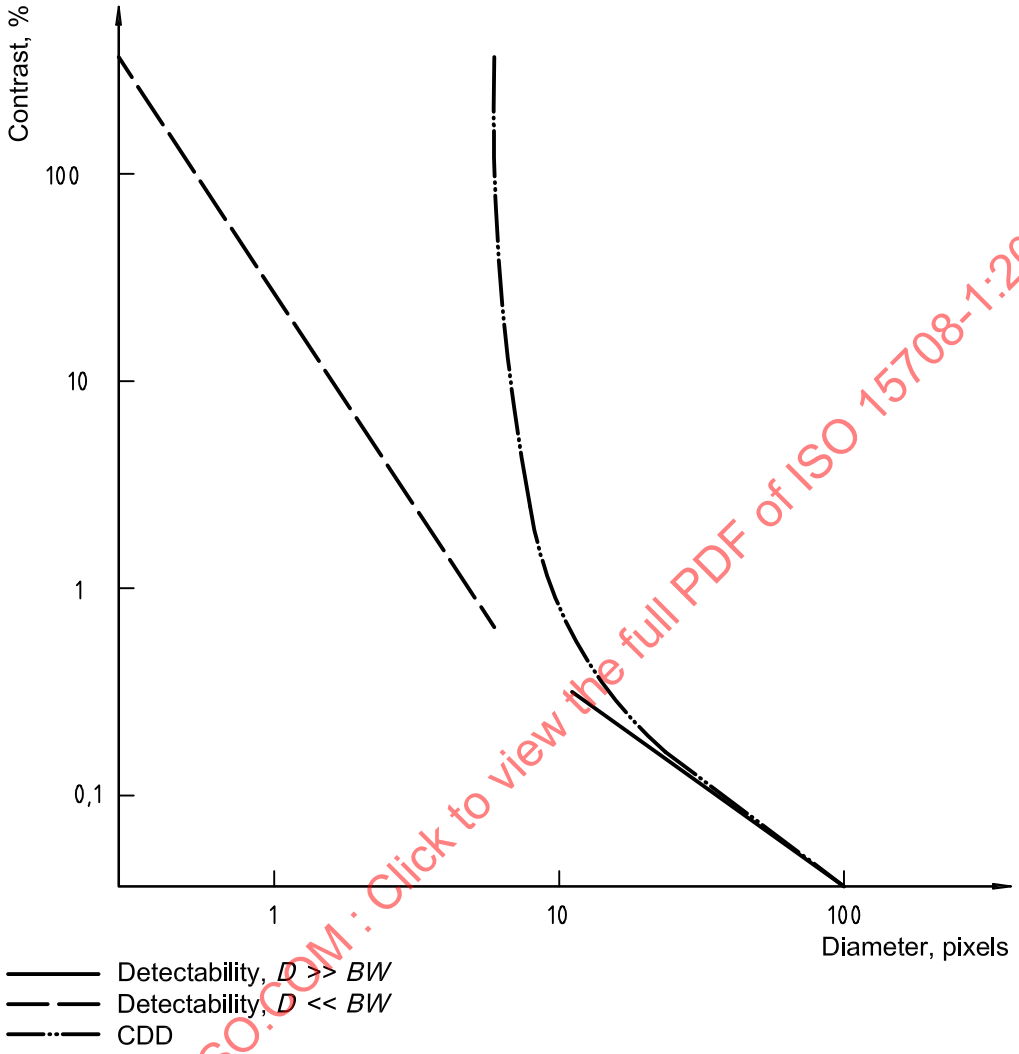

NOTE A value of 8,5 was used for the constant c in equation 22 and its derivative equations.

Figure 19 — Plot illustrating the application of the detectability lines and the CDD curve for an iron cylinder of of radius 2,54 cm that is irradiated by 0,8-MeV X-ray photons

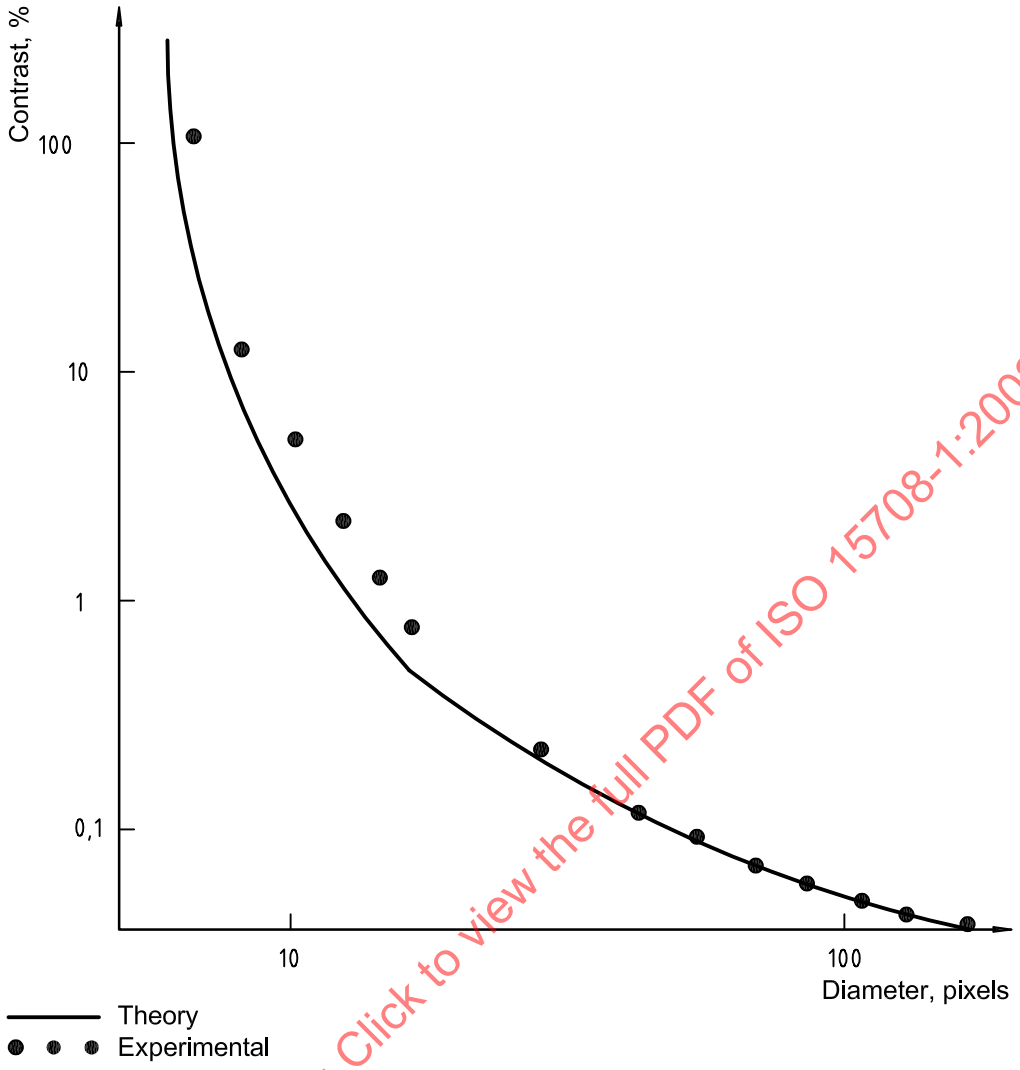

NOTE A value of 8,5 was used for the constant c in equation 22 and its derivative equations.

Figure 20 — Comparison between predicted and measured CDD curves for a real scanner; the object scanned is an iron cylinder of radius 2,54 cm that is irradiated by 0,8-MeV X-ray photons

8 Precision and bias

Computed tomography images are well suited for use in making quantitative measurements. The magnitude and nature of the error in CT-based measurements depends very strongly on the particulars of the scanner apparatus, the scan parameters, the object and the features of interest. Among the parameters which can be estimated from CT images are feature size and shape, feature density contrast, wall thickness, coating thickness, absolute material density and average atomic number.

The use of such quantitative measurements requires that the errors associated with them be known.

NOTE This discussion addresses only the precision and bias of the *measurements*, not the noise or artifact in the images themselves.

The precision of the measurements can best be measured by seeing the distribution of measurements of the same feature under repeated scans, preferably with as much displacement of the object between scans as is expected in practice. This ensures that all effects which vary the result are allowed for; such as photon statistics, detector drift, alignment artifacts, spatial variation of point-spread-function, object placement, and so forth.

One source of such variation in measurements is uncorrected systematic effects such as gain changes or offset displacements between different images. Such image differences can often be removed from the measurement computation by including calibration materials in the image, which is then transformed so that the calibration materials are at standard values. Since air is usually already present in the image, a single additional calibration material (preferably similar to the object material, and placed in a standard position in the image) is often sufficient.

In addition to random variation, measurements of any particular feature may also have a consistent bias. This may be due to artifacts in the image or to false assumptions used in the measurement algorithm. When determined by measurement of test objects, such biases can be removed by allowing for them in the algorithm.

Examination of the distribution of measurement results from repeated scans of test objects with known features similar to those which are the target of the NDE investigation is the best method of determining precision and bias in CT measurements. Once such determinations have been made for a given system and set of objects and scanning conditions, they can be used to give well-based estimates of precision and bias for objects intermediate in size, composition and form, as long as no unusual artifact patterns are introduced into the images.

Annex A
(normative)
Glossary of terms

NOTE This annex contains terms which may be defined in other radiological documents. This glossary provides not only the term definition, but a discussion of the term as it relates specifically to CT.

A.1
afterglow
delayed production of light in a scintillator, which may cause erroneous estimates of X-ray opacity if still significant in amount after the collection time-interval used

DISCUSSION: Afterglow varies substantially between different types of scintillator and is negligible in many CT measurement situations.

A.2
air measurement
reference radiation-intensity measurement made with no object in the examination region of a tomograph

DISCUSSION: Air measurements are used with radiation-intensity measurements through an object to infer opacity. An air measurement is required for each detection element. If the radiation source moves relative to the detection elements, a set of air measurements will generally be required for each source position.

A.3
analytical reconstruction techniques
methods for computing a map of internal CT density from opacity measurements, based on mathematical integration techniques for directly inverting the Radon transform, which the process of measurement approximates.

DISCUSSION: Contrasted to iterative reconstruction techniques. Analytical techniques using Fourier transforms are the basis of almost all commercial CT reconstructions.

A.4
aperture function, detector
three-dimensional function centered on the axis from the radiation source to a detector element, giving the sensitivity of the detector to the presence of attenuating material at each position

DISCUSSION: The detector aperture function gives the extent and intensity distribution of each ray around and along the length of its central line. The function is determined by the size and shape of the radiation source and of the active region of the detector, and by relative distance to the source and the detector. The average width of this function in the region of the object being examined is an important limit on the spatial resolution of a CT scan.

A.5
area detector
X-ray detection apparatus with numerous individual elements arranged in a pattern spread over two dimensions, such as a fluoroscopic screen.

DISCUSSION: This is in contrast to a linear detector array such as used in many tomographic systems.

A.6
artifact – CT
discrepancy between the actual value of some physical property of an object and the map of that property generated by a CT imaging process

DISCUSSION: The term artifact is usually restricted to repeatable discrepancies, with other variations classed as noise. The most common tomographic artifacts result from undersampling the object (where there is object detail finer than the measurement spacing), uncorrected physical effects (such as cupping from beam hardening), and incorrect calibration of detector response or apparatus position.

A.7
attenuation coefficient – X-ray
measure of the rate at which the material in a particular region attenuates an X-ray beam with a particular spectrum as it passes through

DISCUSSION: Of particular relevance to CT is the linear attenuation coefficient, which is the decrease in radiation intensity per unit of distance travelled for a particular substance and radiation-beam composition. Units for this coefficient are typically cm^{-1}. The linear attenuation coefficient is the mass attenuation coefficient multiplied by the mass density of the substance. The CT density in each pixel of a tomogram is basically a linear-attenuation-coefficient value (perhaps with a scaling factor), although artifacts may cause local or global deviations. This coefficient is the sum of the coefficients for several physical attenuation processes (scattering, photoelectric absorption and/or pair production), each of which varies substantially with the X-ray photon energy and the elemental composition of the material. The integral of the linear attenuation coefficients along a ray path gives the X-ray opacity for that ray in the dimensionless natural units called attenuation lengths.

A.8
attenuation length
dimensionless natural unit of X-ray projection values along rays through an object, in terms of the natural logarithm of intensity reduction

DISCUSSION: An opacity of n attenuation lengths implies that the fraction of a photon beam passing through the object without interaction is $1/e^n$. (For multienergetic beams, each energy group is weighted by the signal it generates.)

A.9
attenuation – X-ray
process of reduction of radiation-beam intensity due to interactions during passage through matter

DISCUSSION: Each of the penetrating photons emitted from an X-ray source has a probability of interaction with material in its path dependent on the photon energy and on the thickness, density and elemental composition of the material. Almost all of these interactions will result in the photon being absorbed or scattered so that it will not reach the detector toward which it was originally travelling. The photons remaining in the primary beam are not reduced in energy or changed in any way, thus X-ray beam attenuation is an all-or-nothing process for the individual photons, unlike the gradual loss of energy by each particle in charged particle beams.

A.10
back-projection
process of adding to each pixel a contribution from a (possibly interpolated) value associated with a line through it, as part of the process of reconstruction of a CT-density map of an object from measurements through it

DISCUSSION: The values to be back-projected are derived from groups of measurements, which are usually organized in views, each of which is a projection of the object from one direction. For other than parallel-beam views, a weighting factor (based on distance from the radiation source for fan-beam views) is also used.

A.11
beam hardening
shift in the proportions of the energies in a multienergetic beam of penetrating radiation resulting from the preferential attenuation of the less-penetrating photons

DISCUSSION: The beam photons which pass through an object without interaction are, on the average, more penetrating or “harder” than the original set which entered the object. (Since the penetrating power of X-rays generally increases with energy, hardening usually increases the average energy of the beam.) Failure to correct for the non-linearity in opacity caused by this change in beam composition may cause characteristic “cupping” or “diagonal” artifacts in tomograms. Spectral shifts of this kind can be substantially reduced by suitable beam filtration to remove the least-penetrating portions of the beam.

A.12
beam width
distance normal to the axis of a ray of penetrating radiation over which changes in object opacity will substantially influence the signal generated

DISCUSSION: Typically an average value based on the aperture function in the region of the object is taken to characterize this parameter. The beam width may differ in different directions due to the shape of the source spot or detector aperture. For fan beams, the beam width in the direction normal to the plane of the fan is called the slice thickness.

A.13
Computed axial tomography
CAT
earlier term for what is now known as computed tomography (CT)

DISCUSSION: The term “axial” was used to distinguish the method from focal-plane tomography.

A.14
collimation
restriction of the possible paths for radiation by placement of absorbing material

DISCUSSION: Collimation near the radiation source is used to limit the radiation beam in order to correspond to the general shape of the detection apparatus. In some cases, further collimation near the detector bank or for each detector is used to reduce or eliminate scattered radiation from that which will ultimately be measured.

A.15
Compton scattering
type of interaction between a photon and an electron, in which part of the photon's energy is transferred to the electron as kinetic energy

DISCUSSION: The probability of this type of interaction is proportional to the local electron density. For the range of photon energies and objects used in normal CT scans, it decreases gradually with increasing photon energy, and is generally the most likely mode of attenuation in light materials or at intermediate (0,1 MeV to 10 MeV) photon energies. Also called inelastic scattering.

A.16
computed tomography
CT
non-destructive examination technique in which penetrating-radiation measurements of the X-ray opacity of an object along many paths are used to compute a cross-sectional CT-density map called a tomogram

DISCUSSION: In the original approach, the measurements are planar views made up of overlapping measurements along rays from many regularly-spaced directions, all centered on a slice plane. Approaches using a cone beam have also been developed.

A.17
cone beam
diverging radiation from a source shaped by collimation into a pattern whose dimensions at any given distance from the source are roughly the same in all directions, typically directed at an area detector

DISCUSSION: This is in contrast to a fan beam or a pencil beam.

A.18
cone-beam – CT
use of cone-beam X-ray opacity measurements from many directions to estimate CT density throughout a three-dimensional volume of an object

DISCUSSION: Using two-dimensional area detectors, measurements may rapidly and simultaneously be made through the whole of an object. Such measurements from many directions can be used to compute CT-density values throughout the volume. The speed, efficiency, X-ray energy range, resolution, artifacts, noise and scatter-rejection capabilities of systems utilizing such cone-beam methods can differ substantially from systems using fan-beam methods based on linear detector arrays.

A.19
contrast
extent to which a parameter of interest differs for a certain set of features

DISCUSSION: Thus the contrast in linear attenuation coefficient ("CT density") of aluminum (0,33 cm^{-1}) to iron (1,15 cm^{-1}) is $-0{,}82\ cm^{-1}$, for photons of 200 KeV. Contrast is often stated as the percentage by which the value for one feature is greater or less than the value of the other ("aluminum has a 71 % CT-density contrast to iron at 200 KeV"). Contrasts in the physical properties of different parts of an object may result in contrasts in the image densities for tomograms or radiograms. Since CT density varies with energy quite differently for different materials, the contrast in tomograms can be strongly influenced by beam energy, usually increasing with lower energy. Since image noise usually increases with lower energy even more, image contrast is an incomplete measure of the ease of distinguishing features; see **density resolution** and **contrast-detail diagram**.

A.20
contrast-detail diagram
diagram showing, for a given imaging situation, the contrast at which features of various sizes (and perhaps shapes) can be distinguished with specified confidence

DISCUSSION: Such a CDD summarizes the impact of the noise and blurring in an image on a decision process. Such a diagram is most dependable when it represents empirically-verified tests conducted under actual operating conditions (thus including operator performance and effects specific to a particular inspection task), but diagrams computed from measures of spatial and density resolution can also be useful.

A.21
contrast sensitivity
see **density resolution**

A.22
convolution
transformation of an ordered array of numbers (such as a tomographic view) such that, for each position, a new number is formed from the weighted sum of some of the original numbers, with the weighing factors based only on the amount of difference in position.

DISCUSSION: The array of weighting factors is called a convolution kernel. In most cases the weights decrease with increasing distance; the typical tomographic-reconstruction kernel is $-1/d^2$ for nonzero distances d, with a positive weight at $d = 0$ large enough to make the sum of the weights zero. A process equivalent to convolution can be accomplished efficiently for large kernels with the Fast Fourier Transform (FFT) by multiplying each value of the transform of the data by the corresponding point of a frequency-space filter which is the transform of the kernel. An inverse FFT then converts this product array into the convolved data. The most common methods of tomographic image computation use the FFT to convolve each view of opacity

measurements, and then back-project the resulting filtered line. The $-1/d^2$ kernel transforms into a filter proportional to frequency up to a cutoff frequency determined by the measurement spacing. The precise shape of the filter can be modified to minimize artifacts or to include any other linear filtering desired (see smoothing and sharpening).

A.23
cross-talk
condition in which activity in a measurement channel causes spurious activity in another (usually adjacent) channel

DISCUSSION: This may be due to scattering of radiation in the detector, or to optical or electromagnetic coupling of the signals resulting from detection. Software correction for known cross-talk patterns is often possible.

A.24
CT
see **computed tomography**

A.25
CT density
parameter, related to the action of each region of an object cross-section in attenuating an X-ray beam, which is computed for a two or three-dimensional region by the computed tomography imaging process

DISCUSSION: The term “density” is used in several related but different senses (often without explicit distinction) in reference to CT: e.g. mass density, electron density, optical density and image density, as well as the CT density defined here. For monoenergetic beams, CT density is proportional to the linear attenuation coefficient of each area of the object for the penetrating radiation used for the through-the-object X-ray measurements from which the image is computed. For multienergetic radiation, where the beam spectrum (and thus the attenuation coefficient) passing through each interior point varies with ray direction due to beam hardening, CT densities are averages. In some cases, such as objects made of a single known material, the CT-density measurements or images can be transformed to give values directly in mass density or some other physical parameter which is independent of the energy spectrum of the radiation used for measurement.

A.26
CT-number
quantitative value for CT density, generally based on a linear scale between zero for air and a standard value for a reference material

DISCUSSION: CT-number values for a given object depend on the radiation spectrum as well as the object characteristics, especially for materials of different effective atomic number.

A.27
cupping
artifact in tomographic images, typically due to uncorrected beam hardening, in which the CT-density values in the interior of an object are reduced compared to those near the outside.

A.28
dark measurement
calibration measurement from each detection element made while the radiation source is closed or turned off

DISCUSSION: Dark measurements are used to correct each measurement with that detector. Also called offset measurement.

A.29
density
amount per unit of volume (or, more rarely, of area or length) especially the amount of mass per unit of volume (mass density)

NOTE The term is also used for analogous parameters such as electron density or CT density. A different use of the term is for the dimensionless parameters optical density and film density, measures of attenuation which are the logarithms of transmission ratios.

DISCUSSION: Both usages are relevant in work with radiographic measurements, so adding the appropriate modifier when first using the term or when changing meaning is recommended to avoid confusion. Mass density is often the physical parameter of interest to the investigator in a CT examination; electron density can often be directly inferred from CT scans; CT density (closely related to the linear attenuation coefficient) is the parameter actually measured. In all these cases, a density map over two or three dimensions is used, approximated by values at discrete pixels or voxels. Optical (or film) density refers to a projection along a ray rather than a value at a single point; in fact, digital radiograms are computed density projections in this sense (based directly on the object's transmission of X-rays, not a film's transmission of light). These X-ray projection values which comprise a digital radiogram differ from film-density values in that high values mean less X-ray exposure (zero density is maximum exposure), and in the more dependable relationship between the projection values and the amount of attenuating matter, since exposure time is calibrated for and such sources of variation as film characteristics and development history are avoided.

A.30
density resolution – CT
measure of the extent to which a tomogram or radiogram can be used to detect differences in the physical parameter mapped by the image, for features of a given size

DISCUSSION: The limiting factor in CT density resolution is generally the noise in the image averaged over areas of the feature size; this may vary significantly between different regions of the image. Another important factor is the contrast that the features show under the scan conditions for this image. Taking the ratio of some multiple of the standard deviation of the image noise to a typical image density value is a common method for quantifying density resolution. Image artifacts may also limit resolution in certain cases. Note that the size of the feature and all of the factors which influence image noise and contrast (beam energy, object size, scan time, etc.) shall be specified for a comparison of density-resolution values to be meaningful.

A.31
detectability – CT
extent to which the presence of a feature can be reliably inferred from a tomographic inspection image

DISCUSSION: CT detectability is dependent on the spatial resolution and density resolution of the image, as well as the levels of confidence required in order that false positives and false negatives are avoided. Features may be detectable even if they are too small to be resolved, provided their contrast after blurring is still sufficient.

A.32
detector
device which generates a signal corresponding to the amount of radiation incident on it

DISCUSSION: CT detectors are usually arranged in arrays in one or two dimensions.

A.33
detector spacing
distance (linear or angular) between adjacent radiation collection elements in a detector array

DISCUSSION: In most scanning systems this spacing determines one of the dimensions of the measurement spacing, although some systems use measurement interlacing to overcome this limitation if their detector spacing is large.

A.34
digital radiography
DR
formation of a map of projected X-ray opacity values through all or part of an object by digitalization of signals derived from measurements of penetrating radiation

DISCUSSION: Such X-ray opacity maps can be produced by either a cone beam, used with an area detector such as a fluoroscopic screen or X-ray film, or by moving the object perpendicular to the plane of a fan beam directed at a linear detector array. Differences in scatter rejection, detection efficiency and total detector active area give these approaches quite different characteristics. All DR techniques benefit from the great precision and flexibility in display and analysis that image-analysis software provides. Radiograms made by tomographic

scanners are used both for direct object inspection and as “preview scans” to select the slice planes of interest for CT scans.

A.35
dimensioning accuracy
extent to which the actual dimensions of an object correspond to dimensions calculated from an image, such as a tomogram

DISCUSSION: For objects made of uniform-density materials with smooth surfaces, it is usually possible to obtain dimensions substantially more accurate than the spatial resolution of the image, especially if measurements can be averaged along a surface.

A.36
display matrix size
number of horizontal and vertical pixels available for display of images

DISCUSSION: Display matrix size has no direct connection with the spatial resolution of a tomographic system; however, insufficient display matrix size may require the use of image-zooming techniques to show images at full resolution.

A.37
DR
see **digital radiography**

A.38
dual-energy scanning
use of two sets of measurements through an object taken with differing radiation-beam energy spectra to separate the effects of a mixture of materials

DISCUSSION: Because the variation with beam energy, of the probability for each type of attenuation process is significantly different for most materials, it is possible to use two different energy measurements along the same path in an object to solve for energy-independent physical parameters such as electron density and average atomic number. A common technique is to solve for the amounts of each of two predetermined basis materials whose mixture would give the pair of measurements seen. The separated energy-independent values derived from the measurements can be used to form separate maps (either tomograms or radiograms) of each basis material.

A.39
edge response function
ERF
graph of CT density across an edge, which shows how faithfully the image of a sharp edge is reproduced in a tomogram

DISCUSSION: The image of an edge proceeds in an “S-curve” from a background value through intermediate values (due to partial volume effects or reconstruction artifacts) to a limiting value (the interior CT density of the object). The width of the intermediate region is a good measure of the spatial resolution of an image. For images with little edge artifact, such as tomograms of low-opacity cylinders, the derivative of the edge response function is a good approximation to the line-spread function or point-spread function. The normalized Fourier transform of the point-spread function yields the modulation transfer function (MTF), which gives the relative frequency response of the imaging process.

A.40
elastic scattering
interaction between a photon and a bound electron in an atom, in which the photon is redirected with negligible loss of energy

DISCUSSION: The electron is not affected, with the recoil momentum being transferred to the atom as a whole. The effect is most pronounced at energies less than the binding energy of the electron and its probability decreases with increasing energy. Also referred to as coherent scattering or Rayleigh scattering.

A.41
electron density
number of electrons per unit volume

DISCUSSION: The ratio of electron density to mass density is roughly constant, gradually decreasing from about 3,0 × 1 023 electrons/gram for light elements (except hydrogen, which is twice this value) to 2,4 × 1 023 for the heaviest ones. Because Compton scattering (the dominant attenuation process in many tomographic scans) is directly proportional to electron density, many tomograms are actually maps of electron density.

A.42
false negative
erroneous assertion of the non-existence of a condition (such as a defect) by a decision process, often due to the limited resolution of a tomographic image

DISCUSSION: See **false positive**.

A.43
false positive
erroneous assertion of the existence of a condition (such as a defect) by a decision process, often due to noise or artifact when interpreting tomographic images.

DISCUSSION: The incidence of false positives ("false alarms") depends on the decision criteria as well as the image; e.g. decreasing the sensitivity of the process will generally decrease false positives but will increase false negatives. An analysis of the expected cost and incidence of each type of error is required to choose optimal decision criteria for any particular inspection process.

A.44
fan beam
penetrating radiation from a small source, typically directed at a linear detector array, which has been shaped by collimation into a pattern which is wide in one direction and narrow in the orthogonal direction

DISCUSSION: In fan-beam CT systems, each measurement period gives a planar fan of measurements with a common vertex at the beam spot. Depending on the pattern of object motion, these measurements can be directly handled as fan-beam views or distributed into parallel-beam views. Contrasted to cone beam and pencil beam collimation.

A.45
filter – beam
uniform layer of material, usually of higher atomic number than the specimen, placed between the radiation source and the film for the purpose of preferentially absorbing the softer radiations

DISCUSSION: Filters are used in CT scanners to reduce dose, scattered radiation and beam-hardening effects.

A.46
filter – mathematical
function of spatial frequency giving weighting factors used to modify each point of Fourier-transformed functions or numeric arrays

NOTE Application of such a filter to x-ray projection values is usually a step in the process of reconstructing CT images.

DISCUSSION: Use of such a filter with an FFT is a common way of implementing a convolution. The filter is the Fourier transform of the corresponding convolution kernel.

A.47
focal spot
region at which the electrons are focussed in an X-ray machine or linear accelerator.

DISCUSSION: The size of the resulting beam spot as seen from the object region is an important determinant of the aperture function, especially in the region near the radiation source. Since the spot does not generally have a sharp edge, quantitative values for spot size will reflect the method used to define it, since the average radius of, e.g., the minimum region from which 99 % of the emission comes will be much larger than, say, the standard deviation of the intensity distribution.

A.48
gantry
mechanical apparatus in a tomographic scanner which controls the relative movement of the object to be examined and the source and detector mechanisms

A.49
ionization detector
radiation detector in which the signal is produced by the collection of free electrons or ions directly produced by the radiation beam

DISCUSSION: Examples include xenon gas detectors and semiconductors such as mercuric iodide.

A.50
iterative reconstruction techniques
successive-approximation methods using X-ray opacity measurements for computing an object description (typically a map of some density parameter), based on sequential adjustments of the description to make it consistent with the measurements

DISCUSSION: Algebraic reconstruction techniques (ART) are of this type. Contrasted with analytical reconstruction techniques.

A.51
kernel
set of numerical weights used in the convolution stage of the image-reconstruction process

DISCUSSION: The kernel and the associated frequency-space filter are Fourier transforms of each other.

A.52
keV
kilo-electron-volts, a measure of energy

DISCUSSION: The photons used in industrial CT range in energy from a few keV to several thousand keV.

A.53
kV, kVp
kilovolts, a measure of electrical potential

DISCUSSION: CT beams are often formed by accelerating electrons onto a metal target over voltages ranging from a few tens of kV up to several thousand kV. In each such case, the Bremsstrahlung (braking radiation) photons formed by collisions in the target will range in energy from very small values up to a value in electron volts equal to the accelerating potential in volts.

A.54
laminogram – computed
map of CT-density estimates of an object at positions on a two-dimensional surface, formed by back-projecting radiographic data (perhaps after mathematical filtering) on to the surface.

DISCUSSION: Typically some blurred off-surface features remain in a laminographic image. The advantage of the technique is the ability to produce localized three-dimensional CT-density estimates from substantially less

data than would be required for full three-dimensional reconstructions. Similar in many respects to the analogue process of focal-plane tomography.

A.55
limited-data reconstruction
tomogram formed from an “incomplete” data set in which the object is sampled substantially more in some areas or directions than in others

DISCUSSION: Many forms of data limitation have been dealt with by special methods, including these types of reconstructions: few-angle (large angular steps between views), limited-angle (views missing over some range of directions, as when scanning a wall), limited-field (some portion of some views missing, typically due to high opacity or to positioning constraints) and region-of-interest (views consist of measurements through only a portion of the cross-section).

A.56
line-spread function
see **edge response function**

A.57
linear attenuation coefficient
measure of the fractional decrease in radiation beam intensity per unit of distance travelled in the material (cm^{-1}).

DISCUSSION: The value of this parameter at each point in an object being examined by penetrating radiation depends on the composition of both the material and of the radiation beam passing through that region, as well as the density of the material. Units for this coefficient are typically cm−1. The linear attenuation coefficient is the mass attenuation coefficient multiplied by the mass density of the substance. The CT density in each pixel of a tomogram is basically a linear-attenuation coefficient value, although artifacts may cause local or global deviations. This coefficient is the sum of the coefficients for several physical attenuation processes (see scattering, photoelectric absorption and pair production), each of which varies substantially with the photon energy and the elemental composition of the material. The integral of linear attenuation coefficient along a ray path gives the X-ray projection value for that ray, which is measured in the dimensionless natural units called attenuation lengths.

A.58
linear detector array
array of radiation-sensing elements arranged in a one-dimensional sequence, typically uniformly spaced along an arc or straight line

A.59
magnification
increase in the distance between rays as they proceed from the object to the detectors

DISCUSSION: Equal to the source-detector distance (SDD) divided by the source-object distance (SOD). Large magnifications are made practicable by the use of microfocus X-ray tubes, which give a very compact aperture function close to the source.

A.60
mass attenuation coefficient
measure of the fractional decrease in radiation beam intensity per unit of surface density $cm^2 \cdot g^{-1}$.

DISCUSSION: The value of this parameter at each point in an object being examined by penetrating radiation depends on the composition of both the material and of the radiation beam passing through that region. This coefficient, which is typically expressed in units of cm^2/g, is independent of the density of the substance; that is why it is generally what is given in tables rather than the related linear attenuation coefficient, which is the mass attenuation coefficient multiplied by the mass density.

A.61
mean free path
average distance travelled by an X-ray photon before it is scattered or absorbed by the material through which it is passing

DISCUSSION: See **linear attenuation coefficient** for a discussion of the factors involved.

A.62
measurement interlacing
tomographic scanning pattern of object motion and data reordering in which a finely-spaced fan-beam view is formed by interlacing a set of more coarsely spaced fans with a common vertex

A.63
measurement spacing – CT
angular and linear separation between samples in each view and between view angles

DISCUSSION: The measurement spacing is a basic limit on spatial resolution since it determines the scale at which reconstruction artifacts become unavoidable. For a fixed number of measurements, artifacts are generally minimized when the number of views is about equal to the number of measurements in each view. The measurement spacing is usually matched with the width of the aperture function to give samples which partially overlap but are still mostly independent.

A.64
modulation
extent to which the imaged densities of adjacent features of a given size or spacing are resolved in an image, expressed as a percentage of the actual density contrast

DISCUSSION: Used in specifications of spatial resolution to state the permitted amount of blurring at the specified line spacing.

A.65
modulation transfer function
MTF
function giving the relative frequency response of an imaging system

DISCUSSION: The MTF is the normalized amplitude of the Fourier transform of the point spread function.

A.66
monitor detector
detector used to measure variations in the intensity of the source of penetrating radiation or some other system parameter

DISCUSSION: See **reference detector**.

A.67
monochromatic
alternative term for monoenergetic, when applied to beams of X-rays

A.68
monoenergetic
comprised of photons all having the same energy

DISCUSSION: X-rays and gamma rays produced by the decay of a few radioisotopes, such as americium-241 and caesium-137, are essentially monoenergetic. Many theoretical concepts are defined in terms of monoenergetic beams. See also **multienergetic**.